Trends in Analytical Chemistry 72 (2015) 27–44

Contents lists available at ScienceDirect

Trends in Analytical Chemistry

journal homepage: www.elsevier.com/locate/trac

Advanced materials for optical sensing and biosensing of neurotransmitters

Jafar Soleymani *

Drug Applied Research Center, Tabriz University of Medical Sciences, Tabriz, Iran

ARTICLE INFO

Keywords:
Advanced material
Alzheimer's disease
Bioimaging
Biological fluid
Detection
Neurotransmitter
Optical biosensing
Optical sensing
Parkinson's disease
Schizophrenia

ABSTRACT

Many physiological disorders, including Parkinson's, Alzheimer's and schizophrenia, are associated with variations in the biological levels of neurotransmitters and affect, e.g., learning, sleeping, memory, consciousness, and mood. Real-time, ultrasensitive and accurate detection of neurotransmitter levels in biological fluids not only improves the quality of a patient's life but also can reduce the cost of treatment. Advanced materials can offer remarkable opportunities in the design of bioimaging methods. With advanced materials, hopes of introducing "molecule-sensitive" methods with *in-situ* scientific instrumentation capability increase. This review aims to highlight recent advancements in materials used for detection of important neurotransmitters and focuses on the analytical features of the optical-based methods available.

Contents

Abbreviations: 5-HT, serotonin; AA, ascorbic acid; ACh, acetylcholine; AChE, acetyl cholinesterase; Asp, aspartic acid; ATP, adenosine triphosphate; ATTO-590, $C_{37}H_{39}ClN_2O_9$; BSA, bovine serum albumin; CDs, carbon nanodots; Chox, choline oxidase; CNPs, carbon nanoparticles; CNS, central nervous system; CNTs, carbon nanotubes; CPO-I, 2-(3,5-dinitrophenyl)-4–5-oxazolone; CPO-II, 2-(4-nitrophenyl)-4-[4-(1,4,7,10-tetraoxa-13-azacyclopentadecyl)benzylidene]-5-oxazolone; CPO-III, 2-(4-tolyl)-4-[4-(1,4,7,10-tetraoxa-13-azacyclopentadecyl)benzylidene]-5-oxazolone; CPs, conjugated polymers; DA, dopamine; DBA, DA-binding aptamer; DTSSP, dithiobis(sulfosuccinimidylpropionate); ECL, electrochemiluminescence; EP, epinephrine; GABA, γ-amino butyric acid; GCE, glassy carbon electrode; Glu, glutamic acid; GO, graphene oxide; GSH, glutathione; HB-1, hyper branched viologen polymer; HRP, horseradish peroxidase; ITO, indium tin oxide; Lac, laccase; LCG, lucigenin; LOD, limit of detection; MBA, 4-mercaptophenylboronic acid; MPN, mesoporous silica nanoparticle; MWCNTs, multiwalled carbon nanotubes; NCs, nanoclusters; NEP, norepinephrine; NIR, near infrared; NTA, nitrilotriacetic acid; PAMAM, polyamidoamine; PBS, phosphate buffer solution; PEG, polyethylene glycol; PEI, polyethyleneimine; PMA, polymethacrylic acid; $PPESO_3$, poly(2,5-bis(3-sulfonatopropoxy)-1,4-phenylethynylenealt-1,4-poly(phenylene ethylene)); QDs, quantum dots; RRS, resonance Rayleigh scattering; RSD, relative standard deviation; SAMs, self-assembled monolayers; SERS, surface-enhanced Raman spectroscopy; TGA, thioglycolic acid; UA, uric acid.

* Tel.: +98 9148660544; Fax: +98 4133363231.
E-mail address: jsoleymanii@gmail.com; soleymanij@tbzmed.ac.ir.

http://dx.doi.org/10.1016/j.trac.2015.03.017
0165-9936/

1. Introduction

Neurotransmitters are released from nerves to transmit signals from neurons to a target neuron synapses. Neurotransmitters can be categorized according to their functions into excitatory and inhibitory. The most common excitatory neurotransmitter is glutamate, although glycine and dopamine (DA) have excitatory actions. They convince a nerve cell to produce an action potential, an electrochemical impulse that nerve cells use to transmit signals. In contrast, inhibitory neurotransmitters [e.g., γ-amino butyric acid (GABA) and serotonin (5-HT)] block the signal-transmission process. However, some neurotransmitters possess both properties (e.g., DA). Moreover, some catecholamines, namely DA, norepinephrine (NEP) and epinephrine (EP), play another important role in the central nervous system (CNS) as hormones, and they also affect the regulation of blood pressure, heart rate and lipolysis [1].

Neurotransmitters play important role in many brain functions, including behavior and cognition. They affect and adjust muscle tone and heart rate, and regulate learning, sleeping, memory, consciousness, mood and appetite [2–7].

Changes in the concentration of neurotransmitters in the CNS have been associated with many mental and physical disorders {e.g., Parkinson's, Alzheimer's, schizophrenia, glaucoma, Huntington's, epilepsy, arrhythmias, thyroid hormone deficiency, congestive heart failure, sudden infant death syndrome (SIDS), depression and anxiety [3,4,6,8–17]}. Thus, the quantitative detection of the neurotransmitter in different human fluids appears to be important for diagnosis, monitoring disease state and therapeutic interventions. Table 1 shows the normal concentrations of neurotransmitters in various media.

Real-time and accurate detection of the concentration of neurotransmitters in urine, plasma and cerebral fluids could improve the treatment process and prevent unnecessary drug treatment. So far, more than 100 neurotransmitters have been identified, but this review covers only more common neurotransmitters, including DA, ACh, glutamate, aspartate, GABA, 5-HT, EP and NEP in various physiological mediums (e.g., serum, plasma, urine and cerebral fluids) utilizing optical methods [e.g., fluorescence, luminescence, chemiluminescence, electrochemiluminescence (ECL) and spectrophotometry]. Moreover, it emphasizes figures of merits and most recent materials used in analysis of neurotransmitters.

Numerous methods based on separation-detection methods (e.g., GC, HPLC and CE, electrochemical and flow-injection-based methods) were applied to determine neurotransmitters in various biological environments (Table 2). Although separation-based methods can offer good selectivity and low limits of detection (LODs), they often are costly, require sophisticated equipment, are time consuming and need complex pre-treatment steps. Also, various electrochemical-based methods are very sensitive but their repeatability is poor, while spectroscopic methods are very cheap and rapid and their repeatability is better than electrochemical methods. Also, the sensitivity of most spectroscopic methods is better or comparable with separation and electrochemical-based methods. In the following, there are examples of advanced materials for optical sensing and biosensing of neurotransmitters.

Table 1
Normal concentration of neurotransmitters in biofluids

Neurotransmitter	Medium	Concentration range	Ref.
ACh	Blood	8.66 ± 1.02 nM	[6]
DA	Plasma	0.04–4.50 nM	[17]
GABA	Cerebrospinal fluid	9 ± 5 to 55 ± 27 ng/mL	[18]
NEP	Plasma	0.45–2.49 nM	[19]
EP	Plasma	0.02–0.46 nM	[19]
5-HT	Plasma	101–283 ng/mL	[20]
Glutamate	Plasma	61 μM	[21]

Table 2
Figures of merits of the conventional methods for detection of neurotransmitters

Analysis Method	Type of Analyte	Dynamic range	LOD	Ref.
Spectrophotometric	NEP	1.0–20.0 mg/mL	–	[22]
	EP	0.2–5.0 mg/mL		
	DA	0.4–4.0 mg/mL		
Spectrophotometric	5-HT	0.025–0.5 mM	2.3 μM	[23]
Spectrophotometric	EP	4.8–800 μM	0.26 μM	[24]
	NEP	4.8–600 μM	2.46 μM	
HPLC–MS	NEP	0–4000 ng/mL	9.6 ng/mL	[25]
	EP	0–63 ng/mL	1.9 ng/mL	
	DA	0–1000 ng/mL	6.5 ng/mL	
	5-HT	0–250 ng/mL	0.78 ng/mL	
LSV[a]	5-HT	0.05–10 μM	48 μM	[26]
UFLC–MS/MS[b]	GABA	8.0–4000 ng/mL	–	[27]
	Glu	16–8000 ng/mL		
	NE	4.0–2000 ng/mL		
	DA	4.0–2000 ng/mL		
	5-HT	4.0–2000 ng/mL		
UHPLC-MS/MS[c]	DA	5–1000 ng/mL	2 ng/mL	[28]
	5-HT	5–1000 ng/mL	2 ng/mL	
	NEP	50–1000 ng/mL	20 ng/mL	
	EP	20–1000 ng/mL	5 ng/mL	
	Glu	50–1000 ng/mL	20 ng/mL	
	GABA	50–1000 ng/mL	20 ng/mL	
Amperometry	DA	0.5–50 μM	0.07 μM	[29]
Amperometry	EP	0.5–100 μM	0.07 μM	
SWV[d]	DA	0.5–20 μM	0.1 μM	
SWV	EP	5–100 μM	1 μM	
Chemiluminescence	EP	0.05–1.0 μg/mL	0.03 μg/mL	[30]
	NEP	0.1–1.00 μg/mL	0.05 μg/mL	
	DA	0.1–1.00 μg/mL	0.04 μg/mL	
DPV[e]	DA	0.7–5 μM	0.3 μM	[31]
	5-HT	1–30 μM	50 μM	
LC–MS/MS[f]	ACh	1–250 ng/mL	15 pg/mL	[32]
HPLC	ACh	10–1000 pmol	3 pmol	[33]
MALDI-TOF MS[g]	ACh	1–1000 fmol/μL	0.3 fmol/μL	[34]

[a] Linear sweep voltammetry.
[b] Ultra-fast liquid chromatography/tandem mass spectrometry.
[c] Ultrahigh performance liquid chromatography–tandem mass spectrometry.
[d] Square wave voltammetry.
[e] Differential pulse voltammetry.
[f] Liquid chromatography–mass spectrometry.
[g] Matrix-assisted laser desorption ionization time-of-flight mass spectrometry.

2. Optical sensors and biosensors

2.1. Quantum dots

Quantum dots (QDs), with sizes in the range 2–10 nm, are promising materials for sensitive, precise determinations in biologic media. QDs possess some unique properties (e.g., broad absorption peaks, high-emission quantum yields, narrow and symmetric emission peaks and good chemical and optical stabilities, and their surfaces can be changed to enhance quantum yields).

Mu and co-workers developed a florescence-based method for detection of DA by applying CdSe/ZnS QDs that stabilized with adenosine (Fig. 1). The QDs and DA were connected by nucleotides containing various amino and hydroxyl groups, offering the possibility to interact with DA via non-covalent bonds (e.g., hydrogen bonding and electrostatic interactions). Importantly, adenosine had a negligible effect on the emission profiles and the morphology of the oil-soluble QDs and provided a very stable signal for 24 h in phosphate-buffer solution (PBS) at pH 7.4. DA could be oxidized by ambient O_2 to give dopamine–quinone. The oxidized form of DA acted as an electron acceptor for QDs whose non-radiative emission led to the fluorescence quenching. The DA-QD-based

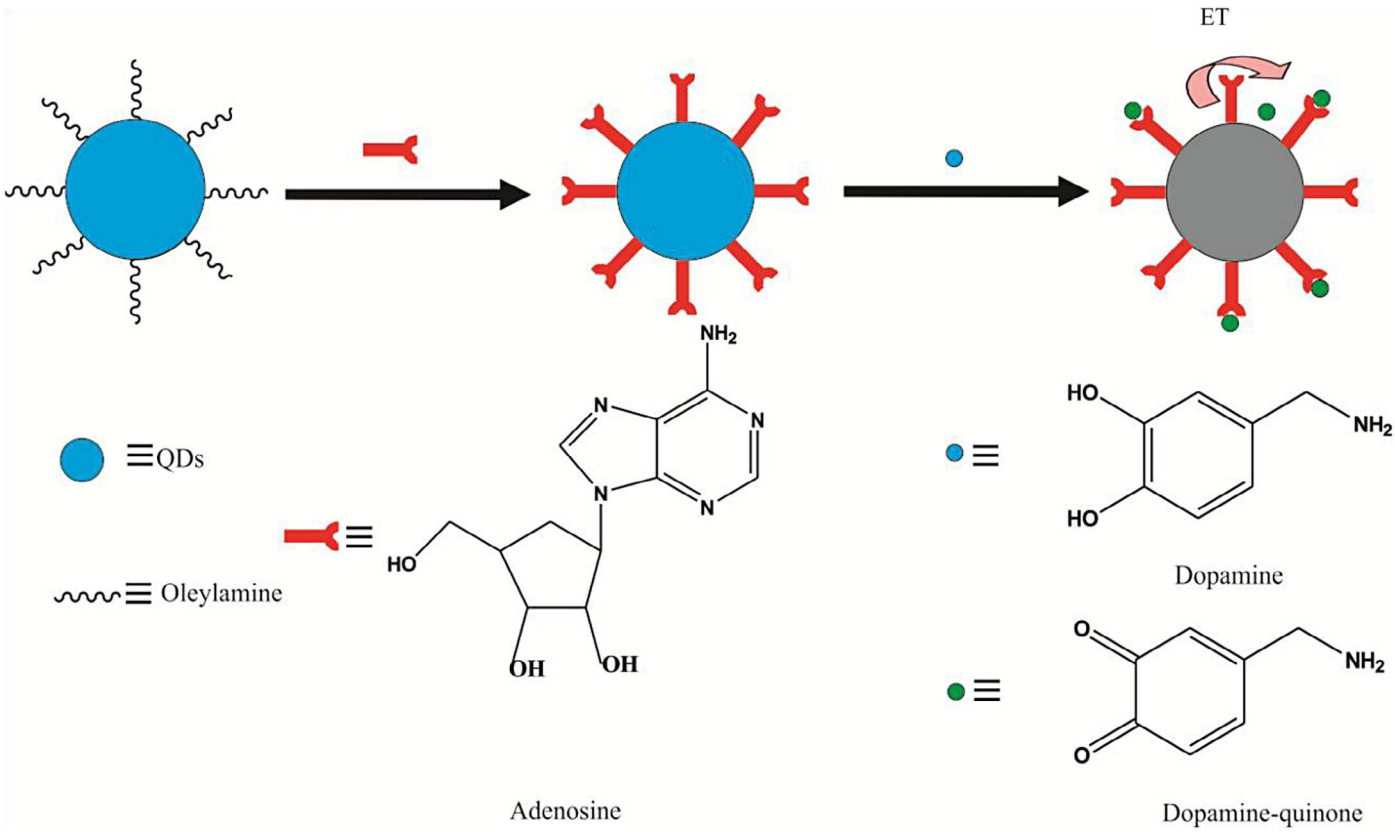

Fig. 1. Fabrication of adenosine-QDs probe and the working principle for the detection of DA.

fluorescence probe showed an LOD of 29.3 nM for DA detection. In 100-fold higher concentrations of coexistent biomaterials [e.g., amino acid, ascorbic acid (AA), uric acid (UA) and glucide], DA was determined with quantitative recoveries 94.8–103.4% [35].

To decrease the toxicity of QDs, $CuInS_2$ ternary QDs were used instead of Cd-containing QDs capped by mercaptopropionic acid. For surface activation, 3-aminophenyl boronic acid molecules were used. The functionalized-$CuInS_2$ QDs containing boronic-acid functional groups were reactive towards vicinal diols to form five or six member cyclic esters in an alkaline aqueous solution. Their actions with fluorescent funcutionalized-$CuInS_2$ QDs caused fluorescence quenching, which could be used as a fluorescent probe for the determination of DA.

The modified funcutionalized-$CuInS_2$ QDs have their own special property [i.e., near-infrared region (NIR) emission wavelength at 736 nm that enables it to get rid of some interferences at lower wavelengths] [36]. These properties are aided by the addition of boronic acid to the raw QDs in changing the emission wavelengths from the original 660 nm to 736 nm. Unlike Cd-based QDs, these QDs have low toxicity for living cells. The stability of the emission light of 3 min can be regarded as the drawback of this method. Also, it seems that the selectivity of this probe is poor due to its sensitivity to the other vicinal diols found in catechol (CA), pyrogallol and gallate [37]. The LOD ($3\delta/s$) for DA was calculated to be 0.2 μmol/L. The linear correlation between quenched fluorescence and the concentration of DA was in the range 0.5–40 μmol/L in human-serum samples.

To provide more biocompatible sensors, silica was used as a modifying agent using its silanol (-SiOH) groups. Also, it effectively stabilizes the QDs in organic and aqueous media. DA can act as an electron acceptor and, at high pH values, its DA-quinone form can bond to QDs by the silanol groups of the QDs and the $^{+}H_3N-$ group of DA-quinone. As mentioned above, the interaction between QDs and the oxidized form of DA leads to quenching of the fluorescence intensity. The method was applied to the determination of DA-spiked human-serum samples in the range 0.0005–0.1 mM (LOD, 2.41×10^{-4} mM), with acceptable recovery values [38].

A combination of CdTe QDs and enzyme was applied as a biosensor of DA in spiked plasma and pharmaceutical samples with an LOD of 0.16 mM. In this study, thioglycolic acid (TGA) was used as a capping agent and the enzyme system of laccase (Lac) catalyzed the oxidation of DA to DA-O-quinone (DOQ), which could selectively quench the strong luminescence of CdTe nanocrystals at neutral pH [39]. At lower and higher pH values, the enzyme activity diminished considerably, also, at very low and high pH values, due to the removal of the TGA from the surface of QDs, luminescence intensity decreased remarkably. As an advantage of Lac system, unlike other enzyme systems, Lac does not require any oxidizing agents that are needed in other similar methods (e.g., H_2O_2 in the peroxidase/H_2O_2 system). The optimum incubation time of 2 min provided a very fast method for DA analysis in the range 0.3–100 mM.

Chen and co-workers exploited a QD-enzyme combination as promising for biosensing of choline and ACh. The fluorescence intensity of the CdTe QDs is diminished by H_2O_2 as a product of the reaction of ACh with acetyl cholinesterase (AChE) to form choline. With application of this method, choline and ACh were analyzed in milk and serum with recoveries about 99%. The LOD of the method for ACh was found to be 10 μM and the linear range was 10–5000 μM. The method is selective to ACh in the presence of glucose, L-lactic acid and ascorbic acid (AA) [40].

Hierarchical-based structures are micro-sized (100 nm) systems that, because of their unique structure-induced optical, electrical, and surface properties, are used in many fields (e.g., photoelectric devices, drug delivery, sensors, filters, coatings, and chemical catalysis) [41]. Sun et al. employed hierarchically-sensitized CdS

aggregates for determination of DA with an LOD of 1.0×10^{-8} M. Quenching of the PL emissions of CdS by DA was expected via the non-radiative pathways aided by the oxidized form of DA. An advantage of these materials is that the quenched fluorescence is located at NIR of 700 nm that is somewhat free from possible interferences [36,42].

Fig. 2 shows a competitive mechanism of sensing of DA and sugar similar to the reported method by Liu et al. [37]. In this study, the glutathione (GSH)-capped CdSe/ZnS QDs were applied to sensing. With addition of 3-aminophenyl boronic acid to the capped QDs, a synthesized probe was sensitized to the vicinal diols that can be found in saccharides and DA. In presence of each other, competitive binding to the CdSe/ZnS QDs proceeded and competition resulted in higher intensities of luminescence. ATTO-590 was used as an acceptor dye to yield the fluorophore-labeled analyte. At 620 nm, upon addition of analyte, the fluorescence of the dye decreased, and the luminescence of the GSH-capped CdSe/ZnS QDs at 570 nm increased, confirming the dynamic exchange of the capping layer with analyte. The reaction time was 30 min for saccharides and DA, and can be regarded as a disadvantage of the reported method. Because the probe can detect other vicinal diols, the selectivity of this material is low [43]. The LOD of the method for determination of DA was reported as 1×10^{-6} M.

Shi et al. used an indium-tin oxide (ITO) paper-based platform for recognition of DA. CdS-QD properties were improved by carbon tapes, which were applied to quantify the concentration of DA in the range 0.001–10 mM [44]. The ECL sensor emitted as a result of the reaction between H_2O_2 and QDs.

Yu et al. dispersed carbon nanotubes (CNTs) into chitosan solution and then CdTe QDs were added to the mixture. The prepared nanocomposite was cast onto the surface of ITO glass and dried using an IR lamp. Emissions of IR improved the stability of the electrode, which could be attributed to the wettability of the cast electrode; also, it improved the morphological characteristics of the layer. In presence of TEA (coreactant), the nanocomposite becomes fluorescent where, by addition of DA, fluorescence intensity decreased in the range 0.05–10 nM (LOD 24 pM). The stability of the ECL sensor was very good with an RSD of 0.34% for seven measurements. In addition, the ECL intensity was somewhat constant after 30 days [45]. Fig. 3 illustrates the mechanism of action of the ECL DA sensor.

Similar work was done by Zhang and co-workers to construct a stepped chemical reaction-based biosensor for analysis of DA in cerebrospinal fluids. After attaching CNTs on the glassy carbon electrode (GCE), boronic acid-functionalized pyrene, DA and 3,3′-dithiodipropionic acid di(N-hydroxysuccinimide ester) (DSP)-functionalized CdTe QDs were added. In the presence of O_2 as coreactant, the CNT/DSP-QD/GCE response was proportional to the concentration of DA in the range 0.05–10 nM (LOD, 26 pM). The selectivity of the probe was good and, in presence of possible coexistent materials (e.g., catechols), the analysis of DA can be done without any obvious interference. Despite selectivity and precision being favorable, the electrode-preparation steps are very sophisticated and the incubation time is very long [46].

In another ECL-based method, Cui and co-workers assayed DA in a drug formulation at NIR region of 695 nm. The water-soluble Ag_2Se QDs were immobilized onto the GCE by applying multi-walled CNTs (MWCNTs) and polyethyleneimine (PEI). The intensity of the fluorescent probe ($S_2O_8^{2-}$ as coreactant) was decreased by adding DA to the medium. The decrease in luminescence of the electrode was linear in the range 0.5–19 μM, and obeyed the fluorescence-quenching principle described by the Stern–Volmer equation. The reported LOD was 0.1 μM, which was not very favorable compared with other reported ECL methods, but its determination in the NIR region is very important due to low possible interference of coexisting materials [36]. Due to the good water solubility and NIR fluorescent emission, this material could be a promising candidate for ECL biosensors, but, as mentioned, the LOD needs to be improved [47].

Bao et al. [48] applied CdSe/ZnS QDs on the GCE for recognition of DA. At optimum conditions, based on the Stern-Volmer equation, fluorescence decreased linearly from 0.1 μM to 20 μM. In

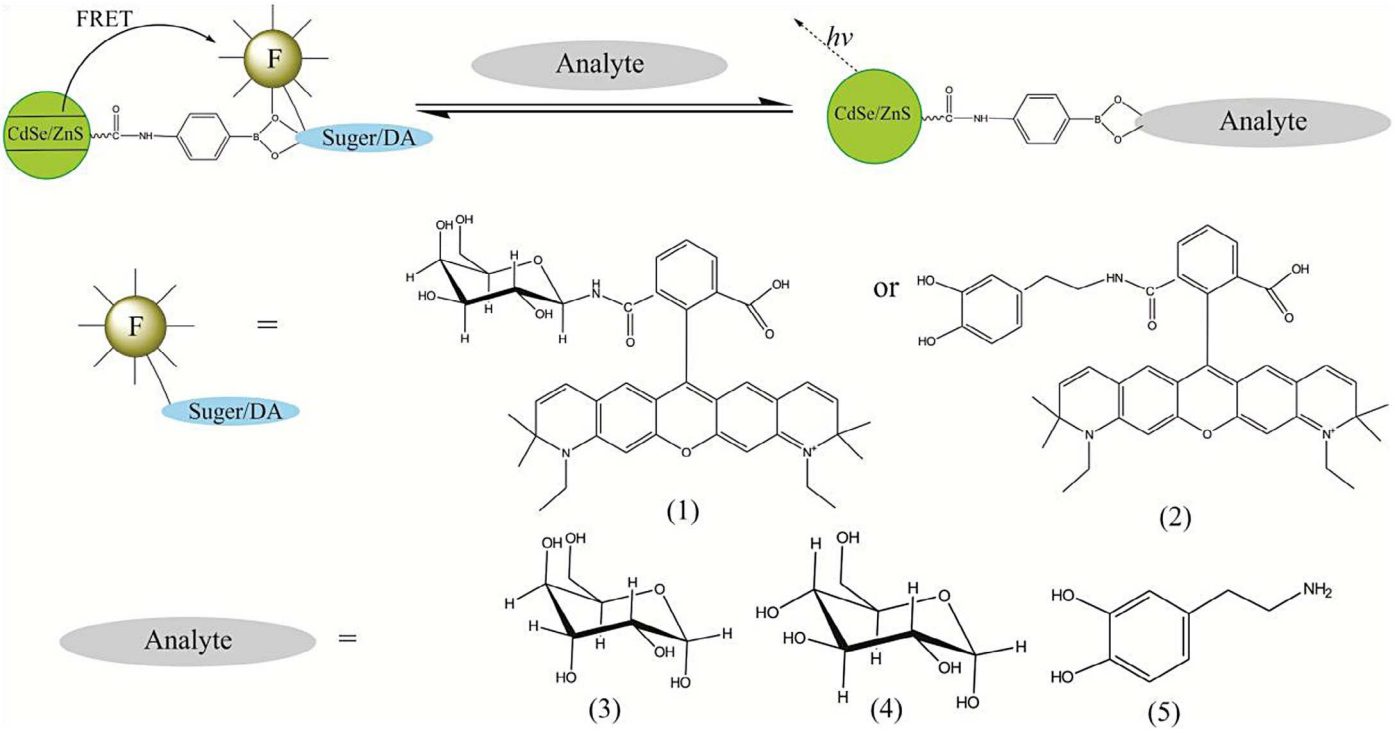

Fig. 2. Competitive detection of dopamine or sugar using ATTO-590 as fluorophore.

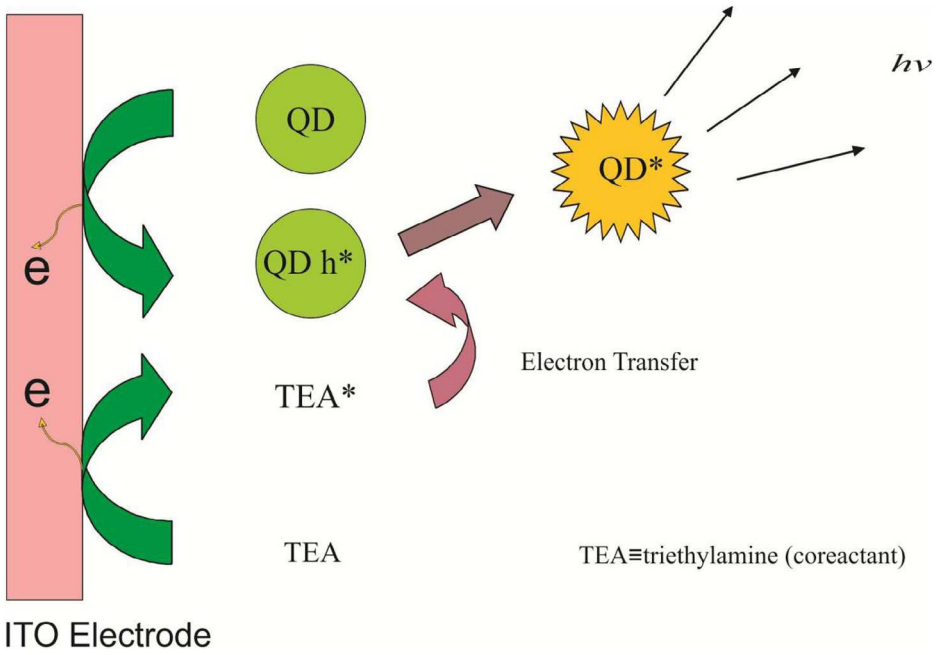

Fig. 3. Mechanism of the DA ECL sensor.

addition, in a similar work by Liu et al. [49] using dual-stabilizer-capped CdSe QDs, DA was detected in drug formulation, human urine, and cerebrospinal fluid samples without any interference from uric acid (UA) and AA. The linear range and LOD were 0.01–3.0 μM and 3.0 nM, respectively. The proposed mechanism of both methods followed the coreactant pathway applying $S_2O_8^{2-}$ as coreactant.

Wang et al. used ZnSe-ferritin nanodot arrays for biosensing GABA by accompanying its conjugation reaction with carboxyl groups of ferritin (Fig. 4). This reaction was done on the 2D-Si substrate with ZnSe-ferritin at pH 7.5 of PBS buffer. After addition of GABA to the substrate solution and incubation for 2 h, the fluorescence intensity increased in proportion to the GABA concentration at 408 nm. The enhanced fluorescence is linear over the concentration range of GABA of 0.03–0.18 μM. Also, the selectivity of the biosensor was tested in presence of Glu as the physiological precursor of GABA, and the results revealed that there was no obvious effect on the fluorescence intensity of GABA from Glu but, at equimolar concentrations, a negligible decrease was observed [50].

Dendrimers are a new class of polymeric materials with regular, highly branched three-dimensional and nanoscale polymeric architectures with a very high density of surface functional groups.

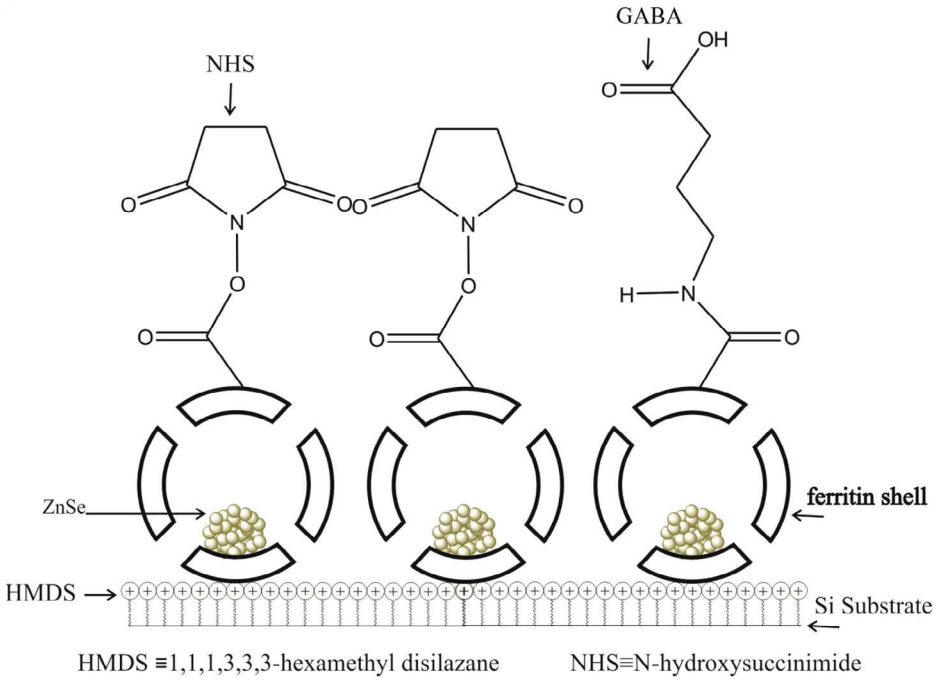

Fig. 4. GABA attached to the ZnSe-ferritin nanodots on modified silicon surface.

Moreover, dendrimers possess unique properties (e.g., high density of active groups, good structural homogeneity, intense internal porosity, and good biocompatibility). Using the superior properties of dendrimers, Sun et al. applied polyamidoamine (PAMAM) as capping ligand for synthesis of CdS QDs, in which PAMAM not only stabilized the CdS QDs but also provided some reactive functional groups for further modifications. In their work, after coating the Au disk with AuNPs, CdS QD/PAMAM was coated on the electrode. With addition of $S_2O_8^{2-}$ (coreactant), the ECL response of the probe was enhanced dramatically. The constructed electrode was applied for determination of DA in urine with dynamic range of 0.05–10 μM and an LOD of 0.012 μM [51]. The reproducibility of the ECL-based sensor was estimated by two measurements with relative standard deviation of 8.6%.

Toxicity of QDs has limited their uses for living cells. Their toxicity depends on multiple factors derived from both inherent physicochemical properties and environmental conditions – QD size, charge, concentration, outer coating bioactivity (capping material and functional groups), and oxidative, photolytic, and mechanical stabilities [52]. Leaching and biodegradation of QDs as a result of mechanical instability release heavy metals to the environment. Coating the outer layer of QDs with epitaxial biocompatible shells (e.g., silica) can increase biocompatibility and reduce leaching of the toxic metal ions from the metalloid core. Also polymers with excellent biocompatibility and low toxicity are successfully and widely employed to modify the surface of QDs and engineer biocompatible QDs for medical and biological applications [53].

2.2. Carbon dots and carbon nanoparticles

Carbon nanodots (CDs) with sizes below 10 nm have attracted attention because of their strong fluorescence, high aqueous solubility, robust chemical inertness, easy functionalization, high resistance to photo bleaching, low toxicity and good biocompatibility [54–56]. We summarize some examples of applications of CDs and carbon nanoparticles (CNPs) in sensing and biosensing of neurotransmitters as follows.

Water-soluble CNPs have excellent photostability and broad-ranging emission spectra. Qu et al. synthesized CNPs from DA with a hydrothermal method and then applied them to determination of Fe^{3+} and DA. By adding DA into the CNP/Fe^{3+} solution at pH 7.0, the fluorescence intensity of the probe increased with concentration of DA (Fig. 5). Unlike some QDs, due to CNPs being non-toxic, these are promising materials for screening of DA in living cells [57]. By employing CNP/Fe^{3+}, DA was analyzed in urine and serum samples with an LOD of 68 nM and linear dynamic range of 0.1–10 μM.

Combinations of MIPs and CDs were used for detection of DA in human spiked urine samples. With application of MIPs, some problems of synthesized CDs (e.g., leaching and permeation) are resolved. Also, their photoluminescence properties are modified by silica-MIPs. The fluorescence intensity of the highly-luminescent CDs@MIP decreased sensitively in the presence of DA molecules. The MIP matrix provided specific binding sites that interacted with the template molecule of DA via non-covalent interactions of hydrogen bonds and van der Waal forces. In contrast with the synthesis of the MIP/QDs, CDs@MIP is synthesized in a one-step reaction. Another advantage of this method is that synthesized CDs@MIP is eco-friendly and is non-toxic [58]. The relative FL intensity of CDs@MIP decreased linearly with increasing DA in the concentration range 25–500 nM with an LOD of 1.7 nM. The spiked urine samples were determined with recoveries of 97.9–102.3%.

2.3. Reduced graphene oxide and graphene oxide

Graphene oxide (GO) is heavily oxygenated, bearing epoxide and hydroxyl functional groups on their basal planes, in addition to carbonyl and carboxyl groups located at the sheet edge, which makes GO a strongly hydrophilic and water-soluble compound. In recent years, GO was one of the materials selected for sensing [59] and biosensing [60,61].

The high fluorescence of GO in acidic solutions makes it an appropriate probe for determining a quenching agent (e.g., DA). Because of the non-covalent interaction between DA and GO, the fluorescence intensity of GO is reduced by adding DA. Selectivity of the NIR-based sensor is more than 15-fold for, e.g., 25 amino acids, sugars, amines, and alcohol [62]. It should be noted that the NIR PL emission of GO is useful for *in vivo* bionanotechnology because of the transparency of body tissues in the NIR 'water window' [63]; also, the NIR region is somewhat free of some possible interferences [36].

By a combination of reduced graphene oxide (rGO) and AuNPs in an rGO/MWCNT/AuNP/GCE electrode, DA was analyzed in injection, serum and urine samples. Upon addition of DA, the luminescence is increased with an LOD (S/N = 3) of 0.067 μM. As reported, the selectivity of the electrode is suitable for detection of DA in the presence of UA, AA, tyrosine, Na^+, K^+, Mg^{2+}, Ca^{2+}, Cl^- or SO_4^{2-} at concentrations of 10 times greater than DA, but EP, NEP, and thyroxine have remarkable fluorescence [64].

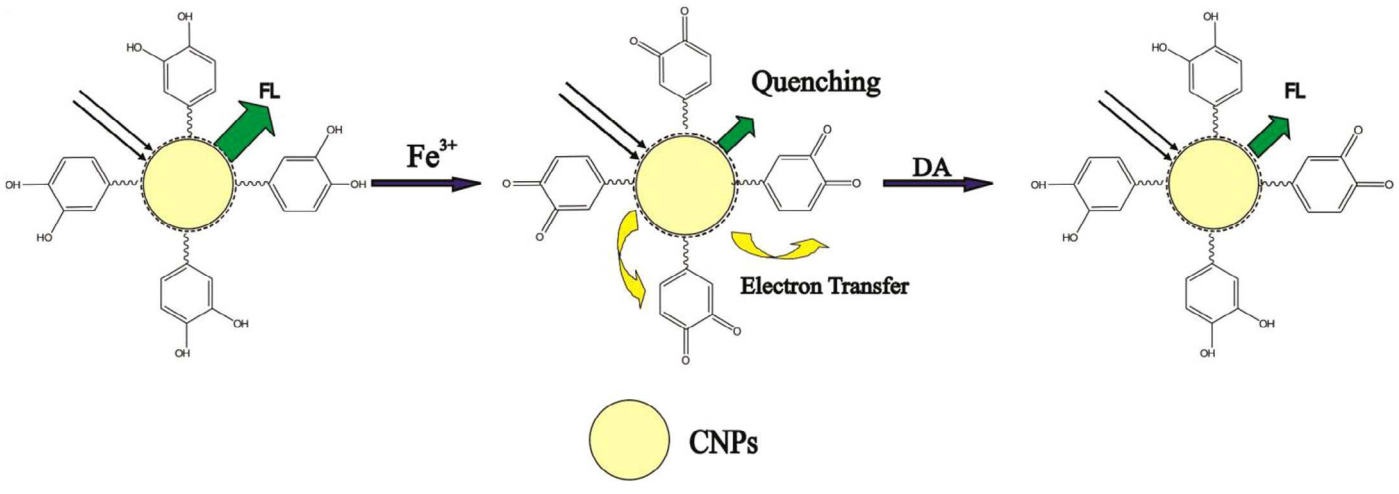

Fig. 5. Mechanism of Fe^{3+} and DA detection by fluorescent carbon nanoparticles.

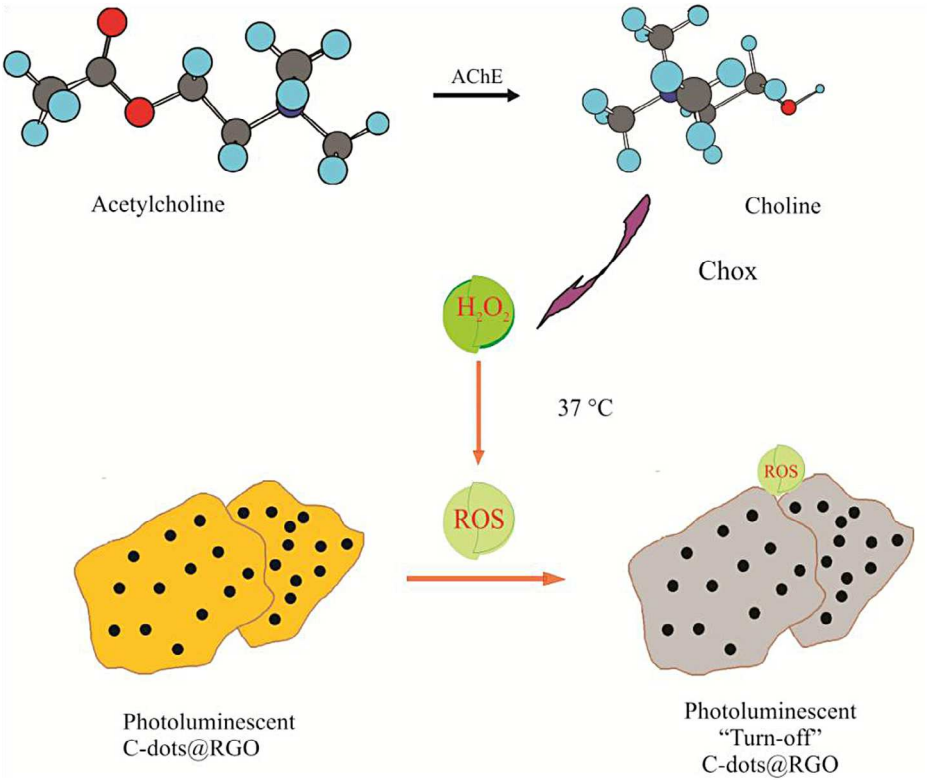

Fig. 6. The detection of ACh by use of photoluminescent C-dots@rGO.

In another work, rGO was used to improve the electrical conductivity of Nafion and tris(2,2′-bipyridyl)ruthenium(II) ($Ru(bpy)_3^{2+}$) nanowires (RuNWs). An ECL sensor was constructed by immobilizing RuNWs onto a GCE with an rGO-Nafion composite [65].

In another work, C-dots were synthesized and deposited on rGO sheets. The highly stable CDs@rGO is a photoluminescent material and its fluorescence decreases with addition of ACh. Initially, ACh was subjected to AChE to produce choline then it was affected by choline oxidase (Chox) enzyme to create H_2O_2 and betaine. Subsequently, reactive oxygen species (ROS) was generated at 37°C to induce more effective fluorescence quenching. The proposed enzyme-based method was applied for detection of ACh in plasma and blood samples [66]. The constructed probe was selective over some possible interferences, including DA, 5-HT, Glu, GABA, glycine, and Asp, whose concentrations are 10-fold greater than the concentration of ACh. The probe possesses some advantages, such as non-toxicity, good stability and selectivity, and has a low LOD. Fig. 6 displays the detection of ACh using photoluminescent CDs@rGO at pH 9.0.

2.4. Nanoclusters

Nanoclusters (NCs) are materials with sizes ranging between atoms and NPs (about less than 2 nm), which can replace organic dyes and QDs [67]. Bovine serum albumin (BSA)-stabilized AuNCs were utilized for assay of DA in injections, human serum and PC12 samples with recoveries of 98.0–102.0%. Upon addition of DA to the BSA-AuNCs, a remarkable decrease in fluorescence intensity occurred at 615 nm. The quenched fluorescence followed the photo-induced electron-transfer mechanism from DA to BSA-AuNCs. Also, with application of this platform along with 3,3′,5,5′-tetramethylbenzidine (TMB) and H_2O_2, the spectrophotometric determination of DA was also assayed at 652 nm. The linear range and LOD for both fluorimetric and spectrophotometric methods were 10 nM–1 mM, and 10 nM, respectively. To investigate the selectivity of the system, possible foreign substances [e.g., AA, UA, 3,4-dihydroxyphenylacetic acid (DOPAC), homovanillic acid (HVA), metal ions (Na^+ and K^+), glucide, and amino acids] were tested and results showed favorable selectivity for DA [68].

Liu et al. reported an ECL method employing the modified ITO electrode with AgNCs immobilized by 3-aminopropyl-triethoxysilane (APTES) and glutaric dialdehyde (GD). Based on formation of the AgNCs@APTES-GD-ITO/DA complex and charge transfer between DA and ITO (coreactant mechanism), the fluorescence intensity increased dramatically. The increased fluorescence intensity was proportional to DA concentration in the range 8.3×10^{-9}–8.3×10^{-7} mol/L and the LOD was 9.2×10^{-10} mol/L at a signal/noise ratio of 3. Using this electrode system in PBS buffer and $S_2O_8^{2-}$, DA was determined in human serum with recoveries of 97.6–101.0% [69].

Interestingly, Li et al. utilized the NCs of Au (Au_{25}) on the ITO electrode for ECL determination of DA in the presence of $S_2O_8^{2-}$ as coreactant. With addition of DA to the PBS buffer at pH 7, the ECL response of the electrode increased dramatically from 2.5 μM to 47.5 μM. Besides the low toxicity of this electrode, excellent stability, good water solubility and acceptable selectivity over UA and AA, the method was not sensitive enough to analyze low concentrations of DA. Unlike QD-based ECL methods, in NC-based ECL methods with addition of DA, the ECL response was enhanced significantly. Fig. 7 shows the ECL mechanism of AuNCs [70].

2.5. Nanowires

Nanowires (NWs) as novel materials are sensitive platforms for realizing single-molecule detection with superior sensing performance. The high surface area-to-volume ratio and the controlled chemical binding make NWs suitable for biosensing {e.g., DNA [71,72], ATP [73], and cholesterol [74]}. Zinc–salophen (ZnSa) is a one-dimensional organic nanostructure, and, along with AgNPs, ZnSA was applied by Chen et al. for analysis of DA in aqueous solution.

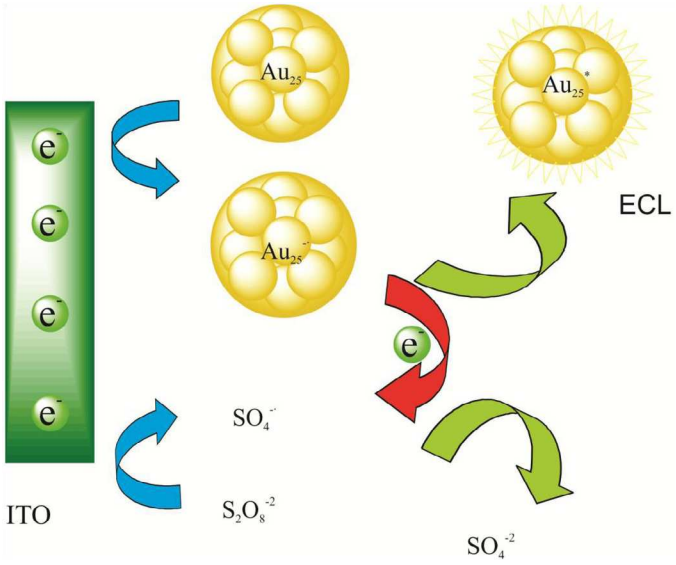

Fig. 7. Mechanism of ECL-DA sensor with applying AuNCs.

As Fig. 8 shows, under UV irradiation, in the absence of DA molecules, all hybrids remained in their original states and displayed a single emission peak at 523 nm, which is the emission peak of ZnSa aggregates. DA acted as a strong donor that could be coordinated and disrupted the surficial aggregated state of NWs, resulting in deaggregation and subsequently release of ZnSa free molecules. Based on this approach, upon addition of DA, another emission band was readily observed at 412 nm, which is just the emission peak of the ZnSa free molecule. Emission in 412 nm is linear over the concentrations of DA of 0–300 nM with an LOD of 3 nM. In contrast with the most reported works, with addition of DA to the hybrid, the fluorescence intensity of the hybrid increased and that can be regarded as an advantage of this method. Because, compared with quenching-based methods, fluorescence-increment methods make it easy to measure low concentrations [75]. The long-term stability of this hybrid can be considered an advantage of this method. Also, due to coordination of DA and ZnSa by $-NH_2$ and –OH groups of DA, it is possible to coordinate with coexisting analytes (e.g., 5-HT) [76].

2.6. Nanoparticles

2.6.1. Gold nanoparticles (AuNPs)

Due to simplicity, high extinction coefficient and strongly distance-based optical properties, AuNPs [77] are suitable materials for colorimetric detection; moreover, by employing AuNPs, one can directly detect analytes by monitoring the color change, using UV–vis spectroscopy, or even the naked eye.

Colorimetric detection of DA based on the interaction between adsorbed Cu^{2+} ions on the surface of AuNPs and functional groups of DA was presented by Su et al. with an LOD of 2×10^{-7} M. Electrostatic adhesion interaction between Cu^{2+} ions with amino group and hydroxyl groups of the DA adsorbed onto the surface of AuNPs causes aggregation of AuNPs, resulting in color change of the solution from wine red to blue. The decreased absorbance showed a linear trend over DA concentrations of 5×10^{-7} M–1×10^{-5} M [78]. In a similar work, the LOD was improved to 30 nM with repeatability of 2.7%. The calibration curve was linear in two ranges of concentration 3.3×10^{-8}–1.0×10^{-7} M and 3.0×10^{-7}–4.5×10^{-6} M. The selectivity of the method is good, as checked using AA as interfering agent [79].

4-Amino-3-hydrazino-5-mercapto-1,2,4-triazol (AHMT)-functionalized AuNPs (AHMP-AuNPs) were used as a model probe for DA analysis. DA increased the absorbance of the probe by acting as a "molecular bridge" between the AHMT-AuNPs and aggregating the AHMP-AuNPs with hydrogen-bond formation (Fig. 9). The method is very simple and cheap but the probe is somewhat sensitive to EP, and that can be regarded as a disadvantage of the method [80]. This method was applied successfully for assay of DA in urine and serum samples in the range 0.20–1.10 μM (LOD, 0.07 μM) with recoveries of 104.6–108.9%.

Zheng et al. used DA-binding aptamer (DBA) instead of AHMP, as DBA can specifically bind to DA to create a selective recognition biosensor for detection of DA in the presence of possible coexisting analytes [e.g., 3,4-dihydroxyphenylalanine (DOPA), CA, DOPAC, HVA, EP and AA]. The citrate-stabilized AuNPs, whose repulsion of anions of citrate prevents the AuNPs from aggregating, lose their stability by adding DA and subsequent formation of DA-binding-aptamer. In the presence of high concentrations of salt (e.g., NaCl) upon addition of DA, the AuNPs change to aggregate form. NaCl would neutralize the negative charge of citrate and lead to the AuNP aggregation. The specific selectivity of the probe arises from the use of DBA, which provides a specific, rigid, framework-like structure. After adding DA, DBA-AuNPs change to aggregate and turn blue. The

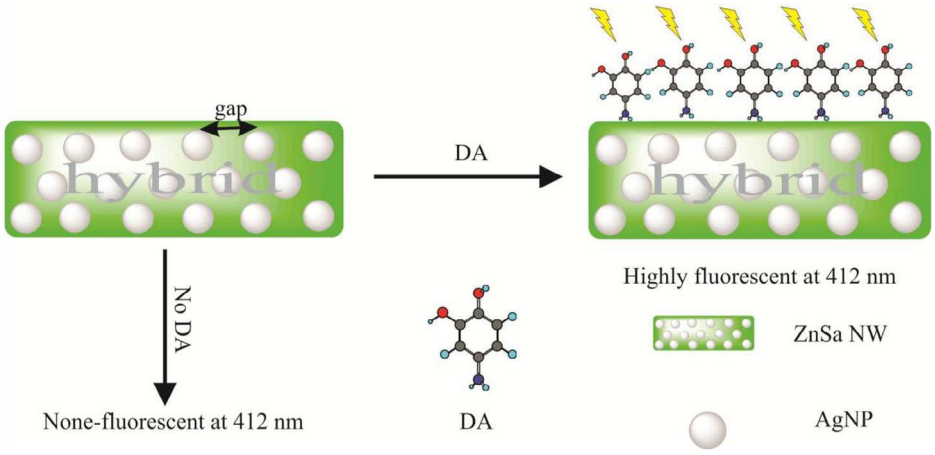

Fig. 8. Zinc–salophen (ZnSa) complex nanowire (NW)–AgNPs 1D hybrid nanostructure for the highly-enhanced fluorescence detection of DA.

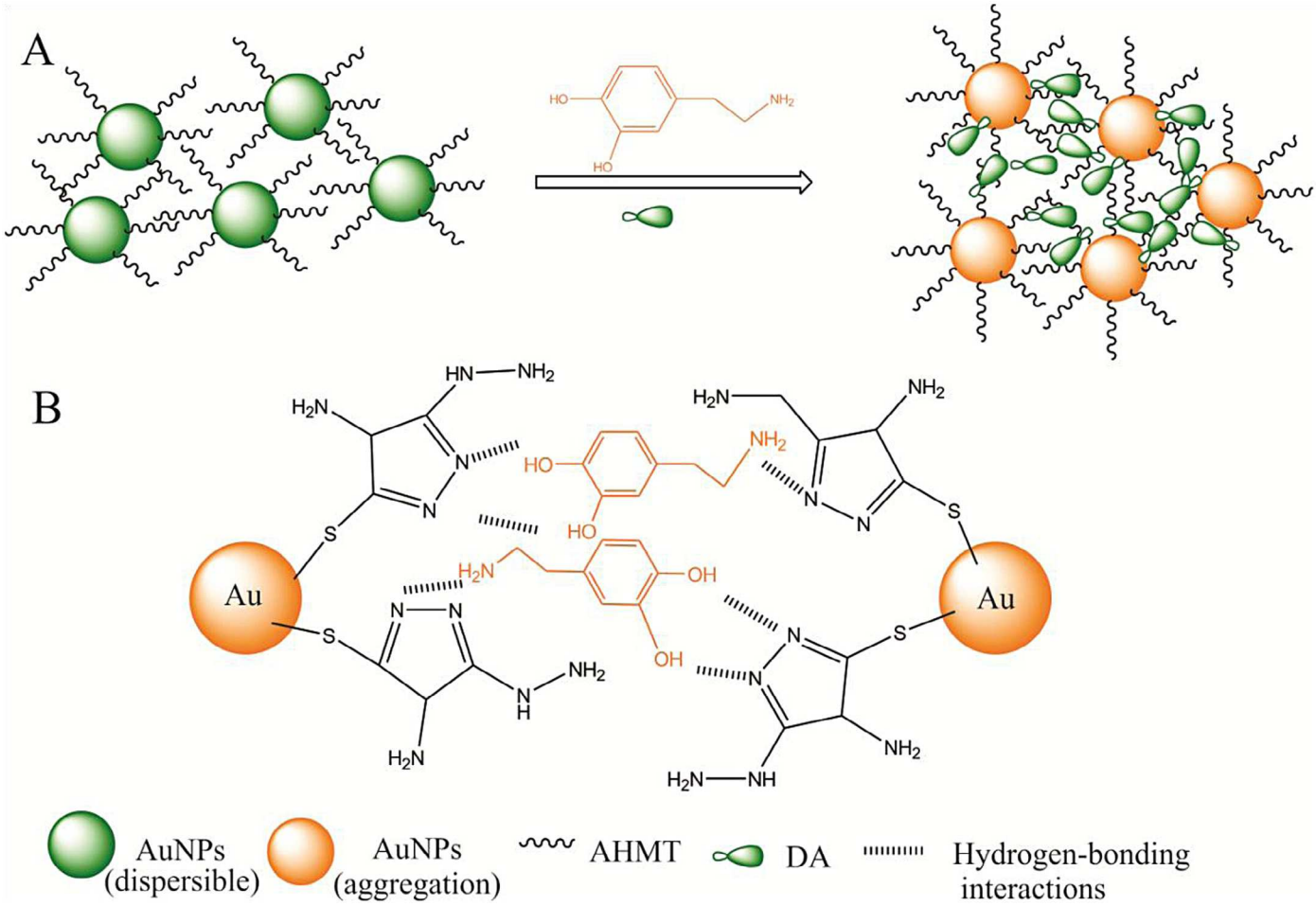

Fig. 9. Colorimetric detection of DA using AHMT-AuNPs as aprobe.

dynamic range and LOD are 0.54–5.4 μM and 0.36 μM, respectively [81].

In another work, a novel material of magnetic Fe_3O_4 particles in combination with dithiobis(sulfosuccinimidylpropionate)-modified AuNPs (DTSSP-AuNPs) was used to create a sandwich-type biosensor for assay of DA at pH 7.2 and room temperature. First, DA molecules were assembled onto the surface of DTSSP-AuNPs via the amine-coupling reaction between the amino group of DA and the activated carboxyl group of DTSSP. Accordingly, DA-DTSSP-AuNPs can be separated from solution by Fe_3O_4 magnetic particles in the presence of an external magnetic field through the interaction of catechol and iron, resulting in a decrease in the color of the DTSSP-AuNPs suspension and a decrease in the UV/Vis absorbance. The decreased absorbance of the probe is linear in the range 0.02–0.80 μM (LOD, 10 nM). Considering that amine-reactive succinimidyl residues on the surfaces of AuNPs can react selectively with the primary amine group of DA, the selectivity of the probe is enhanced in the presence of other catechols and amino acids [82].

Kong et al. [83] described a method based on double molecular recognition for cerebral concentration of DA in rats with an LOD of 0.5 nM. Upon adding DA to the solution containing DTSSP-AuNPs and MBA-AuNPs, a double molecular probe was formed as AuNPs-DTSSP-DA-MBA-AuNPs, and resulted in aggregation of AuNPs. The color of the aggregated AuNPs changed from red to blue, which could be well explained by the DA-induced aggregation of the MBA-DSP-AuNPs through double molecular recognition. Under optimized conditions, a good linear relationship can be found between the absorbance ratio of A_{650}/A_{519} and the concentration of the DA added in the range 5–180 nM.

Unlike other AuNP-based colorimetric detections, Lee et al. developed a very sensitive method based on the etching effect of alkanethiol molecules, which resulted in decreased AuNP size and subsequently a blue shift in the absorption spectra [84]. The results showed that the proposed method achieved an LOD and a dynamic range of 0.5 nM and 10–100 nM, respectively. To check the selectivity of methods, some coexisting materials [e.g., AA, homovanillic acid (HVA), and glutathione (GSH)] were used. Results showed that there are no remarkable effects from possible coexisting materials upon DA detection.

Also, Liu and co-workers [85] reported on a non-aggregating colorimetric sensor based on the effect of DA on the AuNR–Ag^+ system to produce Au-core-Ag-shell NRs (Au@AgNRs). Under pH 9.5, when DA is added to the system, the absorbance changed in proportion to the concentration of the DA because of the redox reaction of DA and Ag^+ in AuNRs–Ag^+ systems. The dynamic range and the limit of quantification (LOQ) of the method were 0.20–12 μM and 0.16 μM, respectively. The proposed sensors with an LOD of 0.047 μM could be used for analysis of DA in biological samples with recovery of 98.0–104.0%. The selectivity of the approach was checked using many coexisting materials (K^+, Na^+, Cl^-, Ca^{2+}, AA, citric acid, cysteine, Asp, Glu, lysine and glucose) with an absolute relative error of lower than 4.6%.

SERS (Surface-enhanced Raman spectroscopy), the increase of Raman scattering by confined electromagnetic fields, possesses many

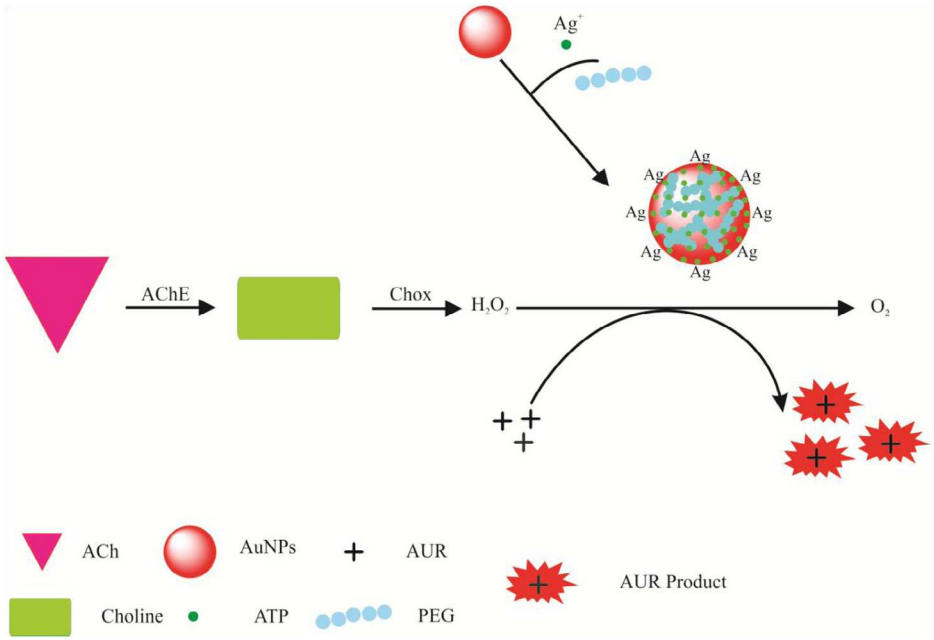

Fig. 10. The sensing strategy of the fluorescent assay using Au/AgNPs to detect ACh.

desirable characteristics as a tool for *in vivo* chemical sensing of biological species, including high specificity, attomole to high zeptomole mass sensitivity and micromolar to picomolar concentration sensitivity [86]. Moreover, due to the narrow bandwidth of SERS spectra, the detection of analyte can be done without any spectral interference. In addition, SERS is very sensitive to minor changes in the structure and the orientation of the molecules. These characteristics, coupled with weak Raman scattering of water, make SERS an ideal technique for analyzing complex biological samples that require little or no sample preparation. Importantly, SERS is achieved using a wide range of excitation frequencies so it can select less energetic excitation (NIR to red) in order to decrease background autofluorescence and photo damage. However, application of SERS in neurotransmitter sensing is very limited and is still at the primary stage of its application [87]. There may be some drawbacks (e.g., the small number of commercially-available SERS-active substrates, their high costs and the difficulty of the interpreting the SERS spectra) that are possible reasons for the limited applications of SERS in neurotransmitter sensing.

More recently, application of the SERS in determination of DA was demonstrated by Lim et al. [88]. In their project, the Raman signal of DA was enhanced by a chitosan-Au nanocomposite anchored on the optical fiber. At first, the surface of the optical fiber functionalized by APTMS and glutaraldehyde ligands and then chitosan NPs were anchored on the surface of the optical fiber. After deposition of AuNPs on the chitosan NPs, the fiber was used as a SERS probe to detect DA in aqueous solution. Amplified Raman signals of DA at 1348 cm^{-1} were proportional in the range 1–10 mM. According to an earlier work of the group [89], chitosan-gold nanoshells were used instead of chitosan-gold nanocomposite anchored on the optical fiber for assay of DA with the same dynamic range at 1382 cm^{-1}. As shown, these methods suffer from low detectability and the probe-preparation steps are complicated.

In research by Choi's group, the possibility of multi-block NRs of Au and Ag for analysis of DA was tested. Initially, the surface of the NRs was modified with monoclonal antibody against DA to sensitize and to specialize the surfaces of NRs. When DA molecules were added to NRs, a red-shift was observed with the magnitude of the peak-shifting ($\Delta\lambda$) and regarded as biosensing signal of localized surface plasmon resonance (LSPR) [90].

In another study conducted by Dutta et al., electropolymerized MIPs on an Au electrode were used for analysis of DA. For this, p-aminostyrene (PAS) as monomer, N,N′-methylene bisacrylamide as cross linker and DA as template were combined as a MIP-SPR sensor for detection of DA. At first, the electropolymerized MIP formed on the surface of the Au transducer, then the SPR signal (reflectivity) was measured at a given angle. With an increase in DA concentration, reflectivity increased linearly. The sensor was sensitive to DA concentration down to 1×10^{-12} M with a response time of about 18 min [91]. The selectivity of probe was tested with tyramine, EP, DOPAC and catechol as coexisting agents in which interference ratios (SPR interference/SPR DA) of 0.09, 0.18, 0.15 and 0.14, respectively, were obtained.

Interestingly, semi-transparent continuous thin Au films were applied by Vaish et al. for sensing of 5-HT. In their research, initially, the surface of the Au film was functionalized by oligo (ethylene glycol) and then 5-HT covalently bound to the self-assembled monolayers (SAMs). Terminal carboxyl groups in the SAMs facilitated the formation of an amide bond between the 5-HT primary amine and the carboxyl groups on SAMs. Substrates were incubated with anti-serotonin primary antibodies and fluorescently-labeled secondary antibodies. The selectivity of 5-HT-functionalized-surface immunosensor was checked in presence of fibronectin, fibrinogen, and BSA, and showed that fibronectin and fibrinogen had no obvious effect on the fluorescence intensity, but, in the presence of BSA, the intensity of fluorescence was decreased about 10% [92].

Wang et al. reported an enzyme-based method for analysis of ACh with an LOD of 0.21 nM. Briefly, Ag^+ ions were attached on the surface of AuNPs by using ATP and PEG. The produced H_2O_2 reacted with non-fluorescent Amplex Ultra Red to form a fluorescent probe in the presence of bimetallic NPs. Fig. 10 shows the mechanism of the ACh biosensor. Results revealed that, in the presence of DA, 5-HT, Glu, GABA, glycine, and Asp, the probe is highly selective toward ACh, mainly due to the high specificity of AChE and Chox toward ACh and choline, respectively. By employing this probe, the amount

of ACh was assayed in serum and blood samples in the range of 1–100 nM [93].

2.6.2. Silver nanoparticles (AgNPs)

Due to the low stability of AgNPs, compared to AuNPs, AgNPs are less utilized for colorimetric detection, despite the AgNPs possessing much higher extinction coefficients than AuNPs of the same size, so stabilized AgNPs can be more versatile than AuNPs. Lin et al. [94] used citrate for stabilizing AgNPs where the stability of AgNPs was caused by the Coulombic repulsive force between the citrate anions.

Fig. 11 depicts the sensing method to analyze DA through the aggregation of AgNPs. Initially, in absence of DA, AgNPs are well dispersed and yellow colored; upon addition of DA, an orange-colored aggregation appears and is attributable to the van der Waals attraction being stronger than electrostatic repulsion between negatively-charged AgNPs. The characteristic peak of AgNPs is located in 392 nm. When DA is added to the mixture, the absorbance decreased and shifted to longer wavelengths. The decreased absorbance shows a linear trend in the range 0–0.6 μM (LOD = 60 nM). The excellent selectivity over the UA and AA is mainly attributed to high-affinity binding between DA and AgNPs via Ag–catechol bonds.

Biswal et al. used a gamma-radiolysis method for synthesis and stabilization of PMA-AgNPs with a simple method that can be done *in situ*. The anionic ions of the deprotonated PMA not only stabilize the AgNPs but also adsorb the free Ag^+ ions on the surface of AgNPs. The adsorbed Ag^+ can subsequently be easily reduced by adding DA, resulting in enhanced absorption at 450 nm. Results showed the response changed linearly with concentration of DA in the range 5.27×10^{-7}–1.58×10^{-5} M with an LOD of 5.27×10^{-7} M. As disadvantages of the method, the selectivity did not test completely and the incubation time for equilibrating of reaction between DA and AgNPs was very high (5 h) [95].

In another work by the Hormozi Nezhad group, the reducing effect of DA was used to synthesize PVP-stabilized AgNPs for spectrophotometry-based sensing of DA, L-DOPA and EP [96]. Also, the group reported simultaneous detection of DA and AA in human serum based on reduction of Ag^+ by DA and AA in the presence of PVP as stabilizer. The SPR changes at 440 nm were recorded and analyzed by three-layered feed-forward artificial neural networks to determine the concentration of each analyte in the mixture [97]. PVP can coordinate with produced H+ and Ag+ to form $Ag(PVP)^+$ and $H(PVP)^+$ complexes, which increase the stability and the production rate of AgNPs. The linear range and LOD for DA were reported as 3.2×10^{-6}–2.0×10^{-5} M and 8.0×10^{-7} M, respectively.

Kaya and his co-worker [98] used an He-Ne laser source (632.8 nm) for activation of iron-nitrilotriacetic acid-attached AgNP [AgNPs-Fe(NTA)]. While the silver core is necessary for enhancing the signal, the Fe(NTA) is used as a trapping agent of DA, whose formation of the ternary complex of NTA-Fe-DA enhances resonance. The SERS intensity enchantment of the probe was recorded at 1480 cm^{-1} with a dynamic range and LOD of 0.5×10^{-9}–4.0×10^{-9} M and 6.0×10^{-11} M, respectively. Interference of AA on the probe showed no obvious effect on the signal of DA, but the effect of other catechols should be checked (because Fe(III) can complex with them to form more stable complexes). This method can be recommended as a rapid and sensitive method for assaying DA (10 s).

Also, Lin et al. [99] evaluated DNA-based AgNPs as a promising material for determination of DA. Initially, DNA-mediated AgNPs were synthesized by adding Ag^+ to ds-DNA in the presence of a reducer (e.g., $NaBH_4$). The nanostructure is sensitive to DA in the presence of Genefinder (GF). Because of the high affinity of the catechol to the Ag, upon addition of DA to the solution, the DNA is released from the structure (Fig. 12), and, subsequently, the reaction of the released DNA molecules with GF resulted in photoluminescence emission at 525 nm. The luminescence intensity was linear in the range of DA concentrations of 1–200 nM with an LOD of 6 nM. The selectivity of this study was good in the presence of the possible foreign substances (e.g., AA, UA, metal ions, glucide, and amino acids).

Lanthanide metals, especially Tb^{3+}, are important sensing materials that provide large Stokes shift, long-time fluorescence emission and narrow emission bandwidth. These specific physicochemical properties of the Tb^{3+} ion make it useful for determination of some pharmaceuticals in serum and urine samples [100,101]. In the presence of AgNPs, Tb^{3+} was used as a fluorophore for determination of catechols in urine, serum and drug formulations with recoveries of 94.5–101.0%. According to unpublished observations in our laboratory, detection of DA without using AgNPs is impossible due to the instability of the fluorescence originating from oxidation of DA in a Tris-HCl buffer solution. By adding AgNPs to the solution of DA, Tb^{3+} and buffer, oxidation of DA is prevented. However, the optimum pH value is 9.0, which is far from the biological pH of around 7.0, so it can be considered a drawback of this method. Also, the reaction time is long enough for rapid analysis of DA [102]. Using the method, the linear dynamic ranges for

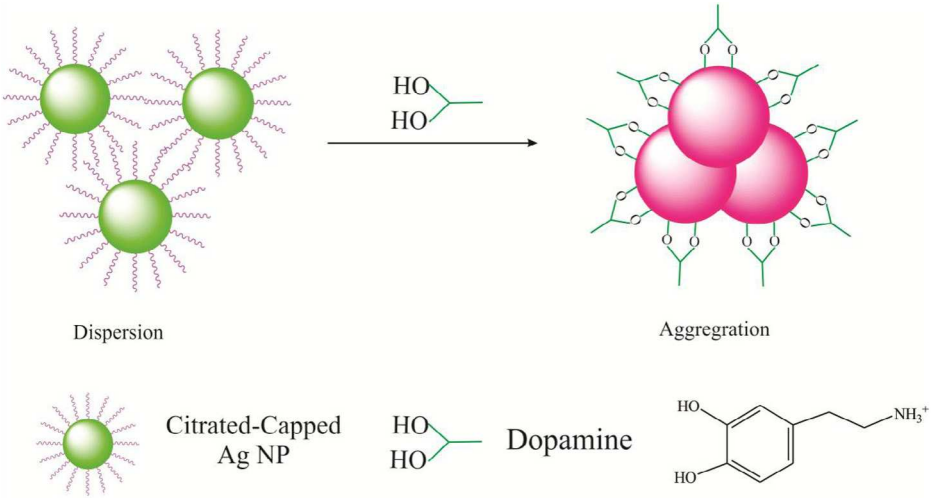

Fig. 11. The colorimetric detection of DA based on AgNPs aggregation.

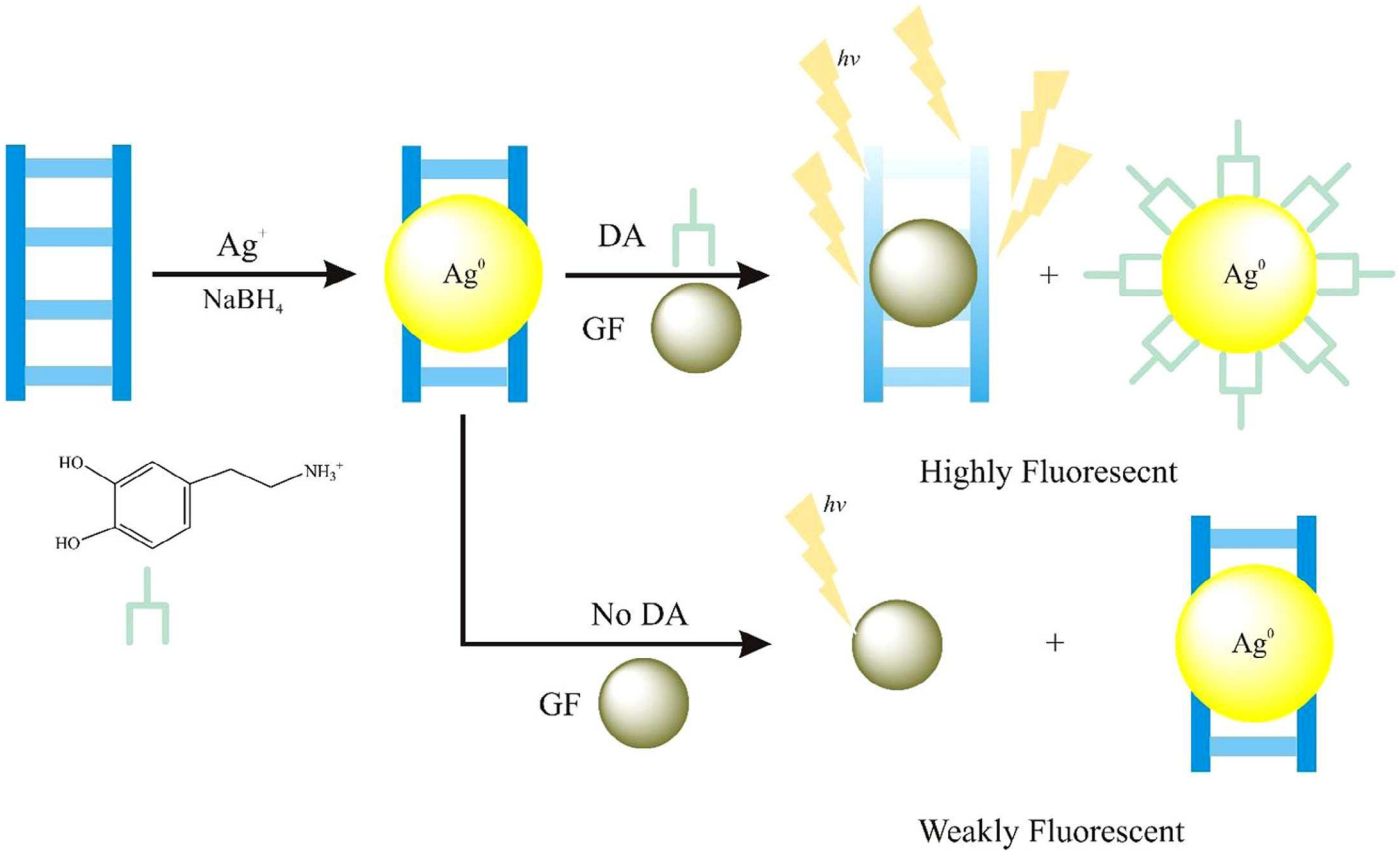

Fig. 12. Strategy for DA determination using DNA-templated AgNPs.

analysis of DA, EP and NEP were 2.4–140 nM, 2.5–110 nM, and 2.8–240 nM with LODs as low as 0.42 nM, 0.25 nM, and 0.64 nM, respectively.

Although AgNP-based nanomaterials are one of favored materials for sensing/biosensing of the neurotransmitters, toxicity is the main problem for *in vivo* detection. AgNP-coated commercial products can potentially leach AgNPs and Ag^+ into the environment. Compared to bulk-silver metal, AgNPs are expected to have higher antimicrobial activity due to their high specific surface area, which releases AgNPs to the environment and can affect the well-being of non-target organisms. Using eco-friendly procedures to produce more stable AgNPs against leaching is of great importance in future studies [103–108].

2.7. Calix(n)arenes

Calix(n)arenes are macromolecular receptors that provide well-defined conformational–structural properties and cavities that are fits for given analytes. Calixarenes immobilize on the surface through aliphatic chains or thiol groups. They have a wide range of applications in sensing, biosensing, biotechnology, and drug discovery, as reviewed by Nimsea and his co-worker [109]. Herein, we review some applications of calixarenes in ACh biosensing.

Korbakov and her associates investigated the possibility of using trans-4-[4-(dimethylamino)styryl]-1-methylpyridinium p-toluenesulfonate (D) and water-soluble p-sulfocalix[n]arenes (C_n) as an artificial receptor for assay of ACh. Upon addition of ACh to the fluorescent complex of C_6D system, because of high affinity to C_6, a substitution reaction occurs between D (chromophore) and Ach, which results in diminished fluorescence intensity of the probe [110]. The response of the complex (n = 6) is linear in the range 5×10^{-8} M–5×10^{-4} M with an LOD of 5×10^{-8} M.

Also, Guo and his research associates reported on the host–guest complexes between C_n (n = 4 to 5) and the cationic aromatic fluorescent dye lucigenin (LCG) for assay of choline and ACh. Like the previous work, by adding the ACh to the C_n-LCG complex, LCG is replaced with the product of the reaction of ACh with AChE to quench the fluorescence intensity of the C_n-LCG complex. The dynamic ranges for choline and ACh were reported as 5–30 μM and 5–20 μM, respectively. The selectivity of the host-guest complex was increased by using enzymatic reactions of Chox and AChE at physiological pH. An advantage of the reported method is that it is possible to determine choline and ACh, both separately and together [111].

In addition, Jin [112] used the complexing ability of calixarenes with rhodamine 800 (Rh800) and indocyanine green (ICG) for photometric detection of ACh in aqueous solution with an LOD of 5×10^{-4} M. Production of complex between Rh800 and calixarenes (S[8]) caused a decrease in the fluorescence intensity of the Rh800. Upon adding ACh to the Rh800-S[8] complex, the fluorescence intensity of Rh800 in the NIR region increased linearly, with the fluorescence intensity of the Rh800-S[8] complex being highly sensitive to ACh over DA, GABA, glysine, and L-aspartate. The competitive displacement between ACh and Rh800 to complex with S[8] caused the fluorescence intensity of Rh800 to increase in the NIR region.

2.8. Polymers

Conjugated polymers (CPs) are other recent materials used for recognizing neurotransmitters. The superior amplification and

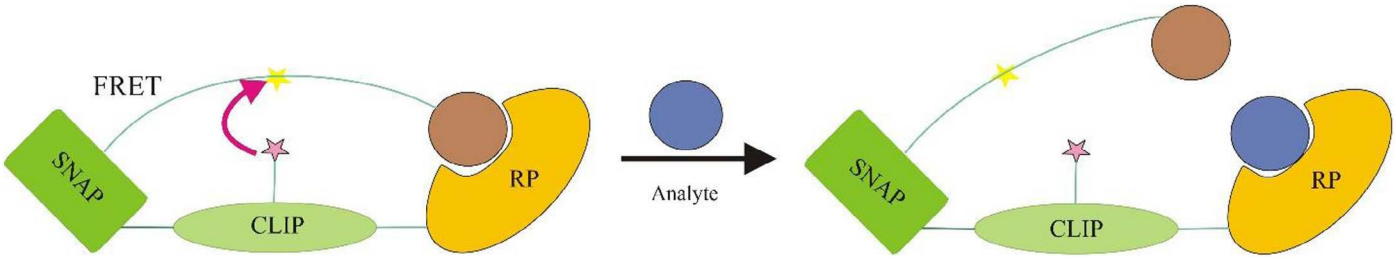

Fig. 13. Structure of Snifit.

quenching properties of CPs enable highly-sensitive detection of many materials, which arises from the CP backbone.

In research presented by Huang et al., $PPESO_3$ polymers along with horseradish peroxidase (HRP) and H_2O_2 were applied for analysis of DA, EP and NEP in human-serum samples with recoveries of 96.3–109.8%. Due to the CP backbone, the fluorescence quenching was more effective. Upon adding catecholamine to the H_2O_2/HRP system, the oxidized form of catecholamines could quench the fluorescence of the water-soluble CP $PPESO_3$ with non-radiative mechanism and the quenched PL intensity ratio (I_0/I) was proportional to the concentration of catecholamine in the ranges 5.0×10^{-7}–1.4×10^{-4} for DA, 5.0×10^{-6}–5.0×10^{-4} for EP, and 5.0×10^{-6}–5.0×10^{-4} M for NEP. Also, the LODs of the method for DA, EP, and NEP were 1.4×10^{-7} M, 1.0×10^{-6} M and 1.0×10^{-6} M, respectively. The $PPESO_3$–HRP-H_2O_2 system was selective for determination of DA, NEP and EP over Na^+, K^+, Cl^-, Ca^{2+}, Mg^{2+}, Zn^{2+}, cysteine and glycine.

CPs have some advantages as biosensors (e.g., compared with QDs, they do not contain lead, cadmium and other heavy metals, which are harmful to the organism, and CPs provide fluorescence amplification and super-quenching properties) [113].

5-HT was detected down to 2 μM using a charge-transfer complex. The complex of hyperbranched viologen polymer (HB-1) and 5-HT was used as acceptor and donor, respectively. The complex formation was checked by UV and fluorescence, with neither 5-HT nor HB-1 showing absorption peaks in the range 400–500 nm. Because of the complex forming, fluorescence intensity at 540 nm and absorption intensity at 430 nm increased in proportion to the concentration of 5-HT up to 20 μM. To increase sensitivity, hyperbranched polymers with high-density viologen units were applied. To demonstrate the selectivity of the method, 5-HT detection was carried out in the presence of L-tryptophan. Interestingly, based on formation of the complex, 5-HT can be simply detected by observing the color change in the solid film. This solid film-based method is very simple in practice, and can be used as a strip sensor for rapid detection of 5-HT [114].

Oztürk et al. [115] constructed reversible fluorescent biosensors for detection of ACh, based on CPO-I, CPO-II and CPO-III derivatives trapped in a PVC matrix and doped with AChE. Trapped AChE on the PVC network catalyzed the hydrolysis reaction of ACh to choline and acetic acid with the changes in the pH value of electrolyte solution being converted to an optical signal by an immobilized dye. The best results were gained by CPO-I biosensor whose quenched fluorescence was linear in the range 1.67×10^{-5}–33.22×10^{-5} M with an LOD of 1.01×10^{-5} M. Although the probe has good reproducibility, reversibility and selectivity, the LOD was not favorable.

2.9. Synthetic proteins

Brun et al. proposed a semi-synthetic fluorescent sensor protein (Snifit)-based florescent method for analysis of glutamate. Snifit is a fusion protein consisting of a SNAP tag as synthetic fluorescent ligand, a CLIP tag as a second synthetic fluorophore, and an analyte-binding protein. Fig. 13 shows the function of a Snifit. As shown, the SNAP tag is labeled with a molecule containing a fluorophore (yellow star) and a ligand (brown ball) that bind to the receptor protein; CLIP tag is labeled with a second fluorophore (purple star). In the absence of analyte, the intramolecular ligand keeps the Snifit in a closed conformation, while, upon adding sufficient concentrations of analyte, the Snifit is shifted toward an open conformation. Opening and closing of the Snifit are detected through changes in FRET efficiency between the two fluorophores. In general, adding analyte to the Snifit system changes the spatial structure or conformation, and results in a change in FRET efficiency. The competition between free analytes and ligand for binding to the binding protein can promote emission intensity and can shift the equilibrium to the open conformation. Excitation of sensor at 547 nm yields a glutamate-dependent emission spectrum between 550 nm and 700 nm that can be exploited for ratiometric sensing [116].

Since GABA does not have a chromophore or a fluorophore and is electrochemically inactive, its detection can be made feasible only via derivatization, but Masharina et al. reported a FRET-based method for detecting GABA on the surface of living mammalian cells using GABA-Snifit as fluorescence sensitive agent. GABA-Snifit contains $GABA_B$ receptor, SNAP tag and CLIP tag, a synthetic fluorophore and a fluorescent $GABA_B$ receptor antagonist. Upon adding GABA to the sensing system, the probe undergoes conformational changes resulting in change to the fluorescence properties of the probe. By applying the Snifit-based probe, GABA is tested on the surface of human embryonic kidney 293 (HEK 239) cells with a dynamic range of up to 10^{-4} M [117].

Poliakov et al. proposed an enzyme-based approach for assay of DA and EP. First, in the presence of enzyme HRP, DA and EP reacted with H_2O_2 and then l-thyroxine was added as an amplification agent to increase the signal of the analyte. The proposed method was linear for DA and EP over concentration ranges 0.5–300 μM and 4–300 μM, respectively. Also, the method was applied to selective detection of catecholamines in pharmaceutical preparations with analysis time of 15 min with the results checked using HPLC-MS [118]. Also, the presence of some coexistence materials (e.g., NaCl, sucrose, fructose, lactose, $Na_2S_2O_5$ and l-cysteine) did not affect the assay of DA and EP.

2.10. Mesoporous nanoparticles

Due to excellent characteristics (e.g., large surface area, recyclable, eco-friendly and functionalization capability), mesoporous silica NPs (MSNs) attracted significant attention for sensing [119], biosensing [120], immunosensing [121] and drug delivery [122]. Yu et al. utilized β-cyclodextrin to enhance the selectivity of an MSN-based biosensor. O-phthalichemithioacetal (OPTA) can react with primary amines to form the fluorescent isoindole product. However, the prevalent amino acids in biological fluids can also react with OPTA, so, to improve the selectivity of the probe, β-cyclodextrin was used. β-cyclodextrin has a unique configuration with a hydrophilic rim and a hydrophobic cavity, and abundant hydroxyl groups

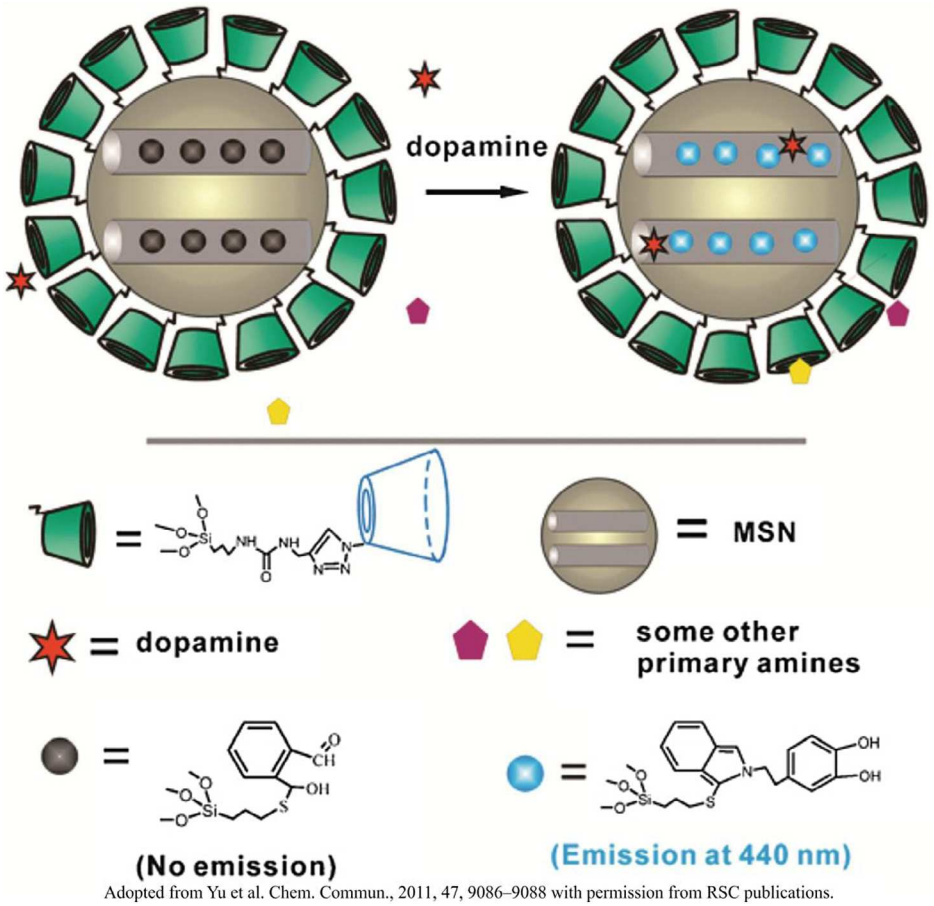

Fig. 14. Mechanism of β-cyclodextrin-modified MSN nanoparticles for selective detection of DA.

on the rim, which can form hydrogen bonds or have polar interaction with the hydrophilic moieties of the amines; these interactions may block some amines, especially those with hydrophilic side groups, from diffusing into the OPTA-modified surface of the MSN. Briefly, the surface properties of MSNs improved with OPTA, which has groups for binding to the primary amines then encapsulated by β-cyclodextrin to enhance the selectivity (Fig. 14). The fluorescence measured at 440 nm is proportional to the concentration of DA in the range 0.05–20 μM with an LOD of 50 nM (pH 7.4, PBS). The selectivity was checked in the presence of 20 common amino acids, and the results showed that histamine and NEP caused great interference in detection of DA. The method is used for detecting DA in serum and urine [123].

2.11. Other materials and nanomaterials

Resonance Rayleigh scattering (RRS) has the characteristics of being simple to perform, low cost, short response time, high sensitivity and convenient. Due to its various beneficial characteristics, it has been extensively applied to determine, e.g., drugs, proteins, and nucleic acids [124–126]. With regard to these features of RRS, Dong et al. utilized zirconium hexacyanoferrate (III) NPs for analyzing DA in a pharmaceutical preparation using the reducing effect of DA. By reduction to zirconium hexacyanoferrate (II), the RRS signal is recorded at 318 nm with RRS intensity being linear over the range 0.03–1.3 mg/mL with a correlation coefficient of 0.9996 and an LOD of 0.392 ng mL^{-1}. The measured RRS signal is constant for about 24 h and the reaction time is 3 min, which is suitable for rapid assay of DA. Because of the reducing effect of some other catechols, AA and UA, it seems that the selectivity of the method can be challenged [127].

Using the method reported by Guo et al. [128], the absorbance of synthesized Prussian Blue [$KFe_3[Fe_2(CN)_6]$] monitored DA concentration in the range 0.05–6.00 μg/mL. Due to the higher apparent molar coefficient (3.2×10^4 L/mol/cm), the present method is very sensitive. The method showed good reproducibility of 0.65% (for 11 determinations) and the LOD was 0.045 μg/mL. The method was used for determination of DA in pharmaceutical preparations, serum, urine and banana with recoveries of 98.6–101.8%. Also, the method is selective with respect to about 25 coexisting materials (e.g., excipients, proteins, carbohydrates and mineral ions).

Interestingly, in another work, the reducing effect of DA was used to reduce $[Fe(CN)_6]^{3-}$ to $Fe_3[Fe(CN)_6]_2$ to form Prussian Blue NPs. By this reaction, a significant enhancement of the RRS intensity could be observed with the enhanced RRS at 350 nm being proportional to the concentration of DA in the range 0.06–10 μg/mL with LOD of 3.43 ng/mL [129]. The effects of inorganic ions, saccharides, amino acids, and proteins on the RRS intensity of DA were investigated at 1.0 μg/mL of DA, results showed that almost all of them have less than 5% interferences but, with Ca^{2+}, NH_4^+, Cl^- and CH_3COO^-, the interference was remarkable.

Das and co-workers [130] reported a chemosensor-based method for analysis of Glu and Asp. As reported, Co(II) complexed with fluorescent ligand of 2-(2-pyridyl)-benzimidazole (PBI) to result in a weakly fluorescent complex with fluorescent quantum yields of 0.024. Upon addition of Glu and Asp to the solution of the Co(II) complex, the fluorescent intensity increased proportional to the concentration of Glu and Asp up to 200 μM. Due to more stable

Table 3
Figures of merits of the reported spectroscopic methods for detection of neurotransmitters

Type of Sensor	Type of Analyte	Determination Method	Dynamic range	LOD	Ref.
CdSe/ZnS QDs/A	DA	Fluorescence	–	29.3 nM	[35]
F-$CuInS_2$ QDs	DA	Fluorescence	0.5–40 μM	0.2 μM	[37]
Cd/Te QDs@silica	DA	Fluorescence	0.5×10^{-3}–0.1 mM	2.4×10^{-4} mM	[38]
CdTe QDs/Lac	DA	Fluorescence	0.3–100 mM	0.16 mM	[39]
CdTe QDs	ACh	Fluorescence	10–5000 μM	10 μM	[40]
CdS aggregates	DA	Fluorescence	–	1.0×10^{-8} M	[42]
CdSe–ZnS QDs-GSH/ATTO-590	DA	Fluorescence	–	1×10^{-6} M	[43]
CdS QDs/ITO	DA	ECL	1 μM–10 mM	–	[44]
CdTe QDs/ITO	DA	ECL	50 pM–10 nM	24 pM	[45]
CNTs/DSP-QDs/GCE	DA	ECL	50 pM–10 nM	26 pM	[46]
Ag_2Se QDs-MWCNT/PEI/GCE	DA	ECL	0.5–19 μM	0.1 μM	[47]
CdSe/ZnS QDs/GCE	DA	ECL	0.1–20 μM	–	[48]
CdSe QDs-ABA/GCE	DA	ECL	10.0 nM–3.0 μM	3.0 nM	[49]
ZnSe nanodots	GABA	Fluorescence	0.03–0.018 μM	–	[50]
CdS-PAMAM-AuNPs/Au	DA	ECL	0.05–10 μM	0.012 μM	[51]
CNPs/Fe^{3+}	DA	Fluorescence	0.1–10 μM	68 nM	[57]
CDs@MIP	DA	Fluorescence	25–500 nM	1.7 nM	[58]
GO	DA	Fluorescence	0.25–20 μM	94 nM	[62]
RGO/MWCNTs/AuNPs/GCE	DA	ECL	0.20–70 μM	0.067 μM	[64]
RGO-Nafion/RuNWs/GCE	DA	ECL	1.0×10^{-12}–1.0×10^{-5} M	3.1×10^{-13} M	[65]
C-dots@RG-Chox-AChE	DA	Fluorescence	0.05–10 nM	30 pM	[66]
AuNCs–BSA	DA	Fluorescence	10 nM–1 mM	10 nM	[68]
AgNCs@APTES-GD/ITO	DA	ECL	8.3×10^{-9}–8.3×10^{-7} M	9.2×10^{-10} M	[69]
AuNCs/ITO	DA	ECL	2.5–47.5 μM	–	[70]
AgNPs–ZnSa	DA	Fluorescence	up to 300 nM	3 nM	[76]
AuNPs-Cu^{2+}	DA	Spectrophotometry	5×10^{-7}–1×10^{-5} M	2×10^{-7} M	[78]
AuNPs-Cu^{2+}	DA	Spectrophotometry	3.3×10^{-8}–1.0×10^{-7} M and 3.0×10^{-7}–4.5×10^{-6} M	30 nM	[79]
AuNPs-AHMP	DA	Spectrophotometry	0.20–1.10 μM	0.07 μM	[80]
AuNPs-BDA-	DA	Spectrophotometry	0.54–5.4 μM	0.36 μM	[81]
DTSSP-AuNPs	DA	Spectrophotometry	0.02–0.80 μM	10 nM	[82]
AuNPs-DTSSP-DA-MBA-AuNPs	DA	Spectrophotometry	5–180 nM	0.5 nM	[83]
AuNPs	DA	Spectrophotometry	$10–10^{+2}$ nM	5 nM	[84]
Au@AgNRs	DA	Spectrophotometry	0.20–12 μM	0.047 μM	[85]
Chitosan-Au nanocomposite	DA	SERS	1–10 mM	–	[88]
Chitosan-gold nanoshells	DA	SERS	1–10 mM	–	[89]
MIP-Au electrode	DA	SPR	–	1×10^{-12} M	[91]
AuNPs-ATP-PEG	ACh	Fluorescence	1–100 nM	0.21 nM	[93]
AgNPs-PMA	DA	Spectrophotometry	Up to 0.6 μM	60 nM	[94]
AgNPs-PMA	DA	Spectrophotometry	5.27×10^{-7}–1.58×10^{-5} M	5.27×10^{-7} M	[95]
AgNPs	DA	Spectrophotometry	3.2×10^{-6}–2.0×10^{-5} M	1.2×10^{-6} M	[96]
PVP/Ag^{+}	DA	Spectrophotometry	3.2×10^{-6}–2.0×10^{-5} M	8.0×10^{-7} M	[97]
AgNPs-Fe(NTA)	DA	SERS	0.5×10^{-9}–4.0×10^{-9} M	6.0×10^{-11} M	[98]
DNA-mediated Ag nanostructures	DA	Fluorescence	1–200 nM	6 nM	[99]
Tb^{3+}/AgNPs	DA	Fluorescence	2.4–140 nM	0.42 nM	[102]
C_6D	ACh	Fluorescence	5×10^{-8}–5×10^{-4} M	5×10^{-8} M	[110]
Calix[n]arenes-LCG	ACh	Fluorescence	5–20 μM	–	[111]
Calixarenes-Rh800	ACh	Fluorescence	–	5×10^{-4} M	[112]
HB-1	5-HT	Spectrophotometry	up to 20 μM	2 μM	[114]
CPO-I	ACh	Fluorescence	1.67×10^{-5}–33.22×10^{-5} M	1.01×10^{-5} M	[115]
Snifit	GABA	Fluorescence	up to 10^{-4} M	–	[117]
H_2O_2-HRP-l-Thyroxine	EP	Spectrophotometry	4–300 μM	–	[118]
MSPs–OPTD	DA	Fluorescence	50 nM–20 μM	50 nM	[123]
Zr[$Fe(CN)_6$] NPs	DA	RRS	0.03–1.3 mg/mL	0.392 ng/mL	[127]
Potassium Ferricyanide-Fe(III)	DA	Spectrophotometry	0.05–6.00 μg/mL	0.045 μg/mL	[128]
$Fe_3[Fe(CN)_6]_2$	DA	RRS	0.06–10 μg/mL	3.43 ng/mL	[129]
Co(II)-PBI	Glu/Asp	Fluorescence	–	up to 200 μM	[130]

complexes of Glu and Asp with PBI, PBI was replaced by Glu and Asp and resulted in increasing fluorescence intensity. The selectivity of the method was tested by the effects of more than 15 amino acids, with no obvious changes in the intensity of Co (II)-Asp or Glu complexes.

3. Conclusions and future outlook

Chemical analysis of neurotransmitters can provide essential information about human health. Neurotransmitters play a crucial role in diagnosis and curing mental disorders, so real-time, accurate detection of their concentrations in various environments is vital.

Herein, we highlighted several recent research breakthroughs on the materials for spectroscopic sensing and biosensing of neurotransmitters in biological media and focused on the figures of merits of the reported research. Surveys of literature showed that many features of materials from nanomaterial to macromolecules were developed for recognition in biological environments of serum, plasma, urine and cerebrospinal fluids.

Nanomaterials improve bimolecular recognition by their large surface area-to-volume ratio, which increases the concentration of biomolecules immobilized onto their surface. As a result, NPs afford an enormous signal increment, related to the high sensitivity of the methods of detection, setting the basis of ultrasensitive detection. The chemical and physical properties of NPs, which are easy to synthesize, to functionalize and to apply to many different branches of sensing, differ from the parent bulk-chemical material, and provide 2D and 3D properties for self-assembly.

QDs and AuNPs are the most common nanomaterials used in sensing and biosensing of neurotransmitters. Cd-free QDs are compatible with *in vivo* detection and provide eco-friendly recognition, and are frequently used. Despite significant advances in detecting neurotransmitters by QDs, more work is required to exploit QD-based sensors and biosensors as tools for *in vivo* detection. For practical uses of *in vivo* detection, more biocompatible, stable, sensitive and repeatable test methods should be developed.

Also, increasing requests for cheap, disposable, analytical, and diagnostic devices convince us to use cheaper, eco-friendly materials [e.g., carbon and its derivatives (graphene, GO, rGO and CDs)]. Their excellent biocompatibility makes them especially attractive candidates for pre-concentration and detection of biological molecules, but application of carbon-based materials for optical sensing of neurotransmitters is still in its infancy with many challenges remaining. One major challenge is their laborious, time-consuming production and there is no scalable production method. Also, their selectivity should be improved through functionalization or hybridization with other groups that have specific affinity for given analytes. Regarding the requests mentioned, it seems that the future of applications of carbon-based materials for optical recognition of neurotransmitter is brighter than for other materials.

From the Table 3, it is clear that the QDs and carbon-based materials are the most sensitive and the best eco-friendly materials for sensing and biosensing of neurotransmitters, respectively. Also, it can be seen that about 70% of research is concerned with DA analysis. From this point of view, it appears that, in future research, QDs and carbon derivatives with improved surface properties and biocompatible features will be applied to test neurotransmitters other than DA. Also, it is clear that most published papers are based on QDs, Au, Ag and carbon compounds, so, in future studies, other NP-based materials will also participate in spectroscopic detection of neurotransmitters.

In brief, the future research trends may include:

1. The presence of multiple compounds, which are closely related; we expect that further developments in materials will open a path to the development of new methods for assay of the simultaneous detection of multiple analytes without any interference from each other.
2. We believe that more biocompatible materials will be produced, able to monitor biological systems in real time and *in vivo*/*in situ*. It seems that nanomaterials can have the main role in obtaining miniaturized, robust, portable devices for *in situ* applications.
3. Taking into consideration the excellent adsorptive properties of carbon compounds, we expect them to play an increasing role in spectroscopic detection of neurotransmitters in the near future.
4. We foresee that other features of nanomaterials (e.g., NCs, nanodots, NRs and NWs), will be take more part in future research.
5. As most reported research suffers from lack of selectivity, we expect research efforts to be focused on improving the analytical figures of merits.

Acknowledgments

The author would like to thank to Professor Abolghasem Jouyban for his support, encouragement and valuable comments.

References

[1] M. Tsunoda, Recent advances in methods for the analysis of catecholamines and their metabolites, Anal. Bioanal. Chem. 386 (2006) 506–514.
[2] R.L. Albin, A.B. Young, J.B. Penney, The functional anatomy of basal ganglia disorders, Trends Neurosci. 12 (1989) 366–375.
[3] A. Grace, Phasic versus tonic dopamine release and the modulation of dopamine system responsivity: a hypothesis for the etiology of schizophrenia, Neuroscience 41 (1991) 1–24.
[4] D.R. Weinberger, B.K. Lipska, Cortical maldevelopment, anti-psychotic drugs, and schizophrenia: a search for common ground, Schizophr. Res. 16 (1995) 87–110.
[5] J.R. Cooper, F.E. Bloom, R.H. Roth, The Biochemical Basis of Neuropharmacology, eighth ed., Oxford University Press, New York, 2003.
[6] W. Xue, T.H. Cui, A high-resolution amperometric acetylcholine sensor based on nano-assembled carbon nanotube and acetylcholinesterase thin films, J. Nano Res. 1 (2008) 1–9.
[7] S.M. Stahl, Mechanism of action of serotonin selective reuptake inhibitors: serotonin receptors and pathways mediate therapeutic effects and side effects, J. Affect. Disord. 51 (1998) 215–235.
[8] J. Castillo, S. Isik, A. Blöchl, N. Pereira-Rodrigues, F. Bedioui, E. Csöregi, et al., Simultaneous detection of the release of glutamate and nitric oxide from adherently growing cells using an array of glutamate and nitric oxide selective electrodes, Biosens. Bioelectron. 20 (2005) 1559–1565.
[9] M. Day, Z. Wang, J. Ding, X. An, C.A. Ingham, A.F. Shering, et al., Selective elimination of glutamatergic synapses on striatopallidal neurons in Parkinson disease models, Nat. Neurosci. 9 (2006) 251–259.
[10] G.K. Isbister, S.J. Bowe, A. Dawson, I.M. Whyte, Relative toxicity of selective serotonin reuptake inhibitors (SSRIs) in overdose, Clin. Toxicol. 42 (2004) 277–285.
[11] D.S. Paterson, F.L. Trachtenberg, E.G. Thompson, R.A. Belliveau, A.H. Beggs, R. Darnall, et al., Multiple serotonergic brainstem abnormalities in sudden infant death syndrome, JAMA 296 (2006) 2124–2132.
[12] C.W. Berridge, B.D. Waterhouse, The locus coeruleus–noradrenergic system: modulation of behavioral state and state-dependent cognitive processes, Brain Res. Brain Res. Rev. 42 (2003) 33–84.
[13] M. Mazloum-Ardakani, H. Beitollahi, M.K. Amini, F. Mirkhalaf, M. Abdollahi-Alibeik, New strategy for simultaneous and selective voltammetric determination of norepinephrine, acetaminophen and folic acid using ZrO_2 nanoparticles-modified carbon paste electrode, Sens. Actuators B Chem. 151 (2010) 243–249.
[14] S.D. Robertson, N.W. Plummer, J. de Marchena, P. Jensen, Developmental origins of central norepinephrine neuron diversity, Nat. Neurosci. 16 (2013) 1016–1023.
[15] J. Grønli, E. Fiske, R. Murison, B. Bjorvatn, E. Sørensen, R. Ursin, et al., Extracellular levels of serotonin and GABA in the hippocampus after chronic mild stress in rats. A microdialysis study in an animal model of depression, Behav. Brain Res. 181 (2007) 42–51.
[16] S. Sirvanci, C.K. Meshul, F. Onat, T. San, Glutamate and GABA immunocytochemical electron microscopy in the hippocampal dentate gyrus of normal and genetic absence epilepsy rats, Brain Res. 1053 (2005) 108–115.
[17] R. Pluto, P. Bürger, Normal values of catecholamines in blood plasma determined by high-performance liquid chromatography with amperometric detection, Int. J. Sports Med. 9 (1988) 75–78.
[18] J. Grove, M.G. Palfreyman, P.J. Schechter, Cerebrospinal fluid GABA as an index of brain GABA activity, Clin. Neuropharmacol. 6 (1983) 223–230.
[19] R.T. Peaston, C. Weinkove, Measurement of catecholamines and their metabolites, Ann. Clin. Biochem. 41 (2004) 17–38.
[20] R.A. McPherson, M.R. Pincus, Henry's Clinical Diagnosis and Management by Laboratory Methods, twenty-second ed., Saunders Elsevier, Philadelphia, PA, 2011.
[21] A. Shinohe, K. Hashimoto, K. Nakamura, M. Tsujii, Y. Iwata, K.J. Tsuchiya, et al., Increased serum levels of glutamate in adult patients with autism, Prog. Neuropsychopharmacol Biol. Psychiatry 30 (2006) 1472–1477.
[22] M. Zhu, X. Huang, J. Li, H. Shen, Peroxidase-based spectrophotometric methods for the determination of ascorbic acid, norepinephrine, epinephrine, dopamine and levodopa, Anal. Chim. Acta 357 (1997) 261–267.
[23] Q. Jin, L. Shan, J. Yue, X. Wang, Spectrophotometric determination of total serotonin derivatives in the safflower seeds with Ehrlich's reagent and the underlying colorreaction mechanism, Food Chem. 108 (2008) 779–783.
[24] M. Sorouraddin, J. Manzoori, E. Kargarzadeh, A. Haji Shabani, Spectrophotometric determination of some catecholamine drugs using sodium bismuthate, J. Pharm. Biomed. Anal. 18 (1998) 877–881.
[25] V. Carrera, E. Sabater, E. Vilanova, M.A. Sogorb, A simple and rapid HPLC–MS method for the simultaneous determination of epinephrine, norepinephrine, dopamine and 5-hydroxytryptamine: application to the secretion of bovine chromaffin cell cultures, J. Chromatogr. B 847 (2007) 88–94.
[26] N.F. Atta, A. Galal, R.A. Ahmed, Simultaneous determination of catecho lamines and serotoninon poly(3,4-ethylenedioxythiophene) modified Pt electrode in presence of sodium dodecyl sulfate, J. Electrochem. Soc. 158 (2011) 52–60.
[27] B. Wei, Q. Li, R. Fan, D. Su, X. Chen, Y. Jia, et al., Determination of monoamine and aminoacid neurotransmitters and their metabolites in rat brain samples by UFLC–MS/MS for the study of the sedative-hypnotic effects observed during treatment with S.chinensis, J. Pharm. Biomed. Anal. 88 (2014) 416–422.
[28] A. Santos-Fandila, A. Zafra-Gómez, A. Barranco, A. Navalón, R. Rueda, M. Ramírez, Quantitative determination of neurotransmitters, metabolites and derivates in microdialysates by UHPLC–tandem massspectrometry, Talanta 114 (2013) 79–89.
[29] A. Salimi, H.M. Khezri, R. Hallaj, Simultaneous determination of ascorbic acid, uric acid and neurotransmitters with a carbon ceramic electrode prepared by sol–gel technique, Talanta 70 (2006) 823–832.

[30] N.T. Deftereos, A.C. Calokerinos, C.E. Efstathiou, Flow injection chemiluminometric determination of epinephrine, norepinephrine, dopamine and L-Dopa, Analyst 118 (1993) 627–632.
[31] G.P. Jin, X.Q. Lin, J.M. Gong, Novel choline and acetylcholine modified glassy carbon electrodes for simultaneous determination of dopamine, serotonin and ascorbic acid, J. Electroanal. Chem. 569 (2004) 135–142.
[32] J. Reubsaet, E. Ahlsen, K. Haneborg, A. Ringvold, Sample preparation and determination of acetylcholine in corneal epithelium cells using liquid chromatography–tandem mass spectrometry, J. Chromatogr. Sci. 41 (2003) 151–156.
[33] J. Ricny, S. Tucek, I. Vins, Sensitive method for HPLC determination of acetylcholine, choline and their analogues using fluorometric detection, J. Neurosci. Methods 41 (1992) 11–17.
[34] M. Persike, M. Zimmermann, J. Klein, M. Karas, Quantitative determination of acetylcholineand choline in microdialysis samples by MALDI-TOFMS, Anal. Chem. 82 (2010) 922–929.
[35] Q. Mu, H. Xu, Y. Li, S. Ma, X. Zhong, Adenosine capped QDs based fluorescent sensor for detection of dopamine with high selectivity and sensitivity, Analyst 139 (2014) 93–98.
[36] J. Thomas, D.B. Sherman, T.J. Amiss, S.A. Andaluz, J.B. Pitner, Synthesis and biosensor performance of a near-IR thiol-reactive fluorophore based on benzothiazolium squaraine, Bioconjug. Chem. 18 (2007) 1841–1846.
[37] S. Liu, F. Shi, X. Zhao, L. Chen, X. Su, 3-Aminophenyl boronic acid-functionalized $CuInS_2$ quantum dots as a near-infrared fluorescence probe for the determination of dopamine, Biosens. Bioelectron. 47 (2013) 379–384.
[38] X. Ai, Q. Ma, X. Su, Nanosensor for dopamine and glutathione based on the quenching and recovery of the fluorescence of silica-coated quantum dots, Microchim. Acta 180 (2013) 269–277.
[39] M. Shamsipur, M. Shanehsaz, K. Khajeh, N. Mollaniad, S.H. Kazemi, A novel quantum dot–laccase hybrid nanobiosensor for low level determination of dopamine, Analyst 137 (2012) 5553–5559.
[40] Z. Chen, X. Ren, X. Meng, D. Chen, C. Yan, J. Ren, et al., Optical detection of choline and acetylcholine based on H_2O_2-sensitive quantum dots, Biosens. Bioelectron. 28 (2011) 50–55.
[41] Y. Cheng, Y. Wang, C. Jia, F. Bao, MnS hierarchical hollow spheres with novel shell structure, J. Phys. Chem. B 110 (2006) 24399–24402.
[42] B. Sun, C. Wang, High-sensitive sensor of dopamine based on photoluminescence quenching of hierarchical CdS spherical aggregates, J. Nanomater. 2012 (2012) 1.
[43] R. Freeman, L. Bahshi, T. Finder, R. Gill, I. Willner, Competitive analysis of saccharides or dopamine by boronic acid-functionalized CdSe-ZnS quantum dots, Chem. Commun. (7) (2009) 764–766.
[44] C.G. Shi, X. Shan, Z.Q. Pan, J.J. Xu, C. Lu, N. Bao, et al., Quantum dot (QD)-modified carbon tape electrodes for reproducible electrochemiluminescence (ECL) emission on a paper-based platform, Anal. Chem. 84 (2012) 3033–3038.
[45] C. Yu, J. Yan, Y. Tu, Electrochemiluminescent sensing of dopamine using CdTe quantum dots capped with thioglycolic acid and supported with carbon nanotubes, Microchim. Acta 175 (2011) 347–354.
[46] L. Zhang, Y. Cheng, J. Lei, Y. Liu, Q. Hao, H. Ju, Stepwise chemical reaction strategy for highly sensitive electrochemiluminescent detection of dopamine, Anal. Chem. 85 (2013) 8001–8007.
[47] R. Cui, Y.P. Gu, L. Bao, J.Y. Zhao, B.P. Qi, Z.L. Zhang, et al., Near-infrared electrogenerated chemiluminescence of ultrasmall Ag_2Se quantum dots for the detection of dopamine, Anal. Chem. 84 (2012) 8932–8935.
[48] L. Bao, L. Sun, Z.L. Zhang, P. Jiang, F.W. Wise, H.C.D. Abruña, et al., Energy-level-related response of cathodic electrogenerated-chemiluminescence of self-assembled CdSe/ZnS quantum dot films, J. Phys. Chem. C 115 (2011) 18822–18828.
[49] S. Liu, X. Zhang, Y. Yu, G. Zou, A monochromatic electrochemiluminescence sensing strategy for dopamine with dual-stabilizers-capped CdSe quantum dots as emitters, Anal. Chem. 86 (2014) 2784–2788.
[50] T. Wang, H.W. Choi, W.J. Kim, J.S. Kim, S.J. Park, Two-dimensional array of ZnSe-ferritin nanodots as a sensor media for gamma-aminobutyric acid, Mol. Cryst. Liquid Cryst. 519 (2010) 27–35.
[51] F. Sun, F. Chen, W. Fei, L. Sun, Y. Wu, A novel strategy for constructing electrochemiluminescence sensor based on CdS-polyamidoamine incorporating electrodeposited gold nanoparticle film and its application, Sens. Actuators B Chem. 166 (2012) 702–707.
[52] K.M. Tsoi, Q. Dai, B.A. Alman, W.C. Chan, Are quantum dots toxic? Exploring the discrepancy between cell culture and animal studies, Acc. Chem. Res. 46 (2012) 662–671.
[53] N. Tomczak, D. Jańczewski, M. Han, G.J. Vancso, Designer polymer–quantum dot architectures, Prog. Polym. Sci. 34 (2009) 393–430.
[54] S.N. Baker, G.A. Baker, Luminescent carbon nanodots: emergent nanolights, Angew. Chem. Int. Ed. Engl. 49 (2010) 6726–6744.
[55] L. Cao, X. Wang, M.J. Meziani, F. Lu, H. Wang, P.G. Luo, et al., Carbon dots for multiphoton bioimaging, J. Am. Chem. Soc. 129 (2007) 11318–11319.
[56] J. Shen, Y. Zhu, X. Yang, C. Li, Graphene quantum dots: emergent nanolights for bioimaging, sensors, catalysis and photovoltaic devices, Chem. Commun. 48 (2012) 3686–3699.
[57] K. Qu, J. Wang, J. Ren, X. Qu, Carbon dots prepared by hydrothermal treatment of dopamine as an effective fluorescent sensing platform for the label-free detection of iron(III) ions and dopamine, Chem. Eur. J. 19 (2013) 7243–7249.
[58] Y. Mao, Y. Bao, D. Han, F. Li, L. Niu, Efficient one-pot synthesis of molecularly imprinted silica nanospheres embedded carbon dots for fluorescent dopamine optosensing, Biosens. Bioelectron. 38 (2012) 55–60.
[59] S. Roy, N. Soin, R. Bajpai, D. Misra, J.A. McLaughlin, S.S. Roy, Graphene oxide for electrochemical sensing applications, J. Mater. Chem. 21 (2011) 14725–14731.
[60] Y. Liu, D. Yu, C. Zeng, Z. Miao, L. Dai, Biocompatible graphene oxide-based glucose biosensors, Langmuir 26 (2010) 6158–6160.
[61] Y. Shao, J. Wang, H. Wu, J. Liu, I.A. Aksay, Y. Lin, Graphene based electrochemical sensors and biosensors: a review, Electroanalysis 22 (2010) 1027–1036.
[62] J.L. Chen, X.P. Yan, K. Meng, S.F. Wang, Graphene oxide based photoinduced charge transfer label-free near-infrared fluorescent biosensor for dopamine, Anal. Chem. 83 (2011) 8787–8793.
[63] S.F. Lim, R. Riehn, W.S. Ryu, N. Khanarian, C.K. Tung, D. Tank, et al., *In vivo* and scanning electron microscopy imaging of upconverting nanophosphors in caenorhabditis elegans, Nano Lett. 6 (2006) 169–174.
[64] D. Yuan, S. Chen, R. Yuan, J. Zhang, X. Liu, An ECL sensor for dopamine using reduced graphene oxide/multiwall carbon nanotubes/gold nanoparticles, Sens. Actuators B Chem. 191 (2014) 415–420.
[65] Q. Li, J.Y. Zheng, Y. Yan, Y.S. Zhao, J. Yao, Electrogenerated chemiluminescence of metal–organic complex nanowires: reduced graphene oxide enhancement and biosensing application, Adv. Mater. 24 (2012) 4745–4749.
[66] C.I. Wang, A.P. Periasamy, H.T. Chang, Photoluminescent C-dots@RGO probe for sensitive and selective detection of acetylcholine, Anal. Chem. 85 (2013) 3263–3270.
[67] M. LisaáPhipps, A DNA-templated fluorescent silver nanocluster with enhanced stability, Nanoscale 4 (2012) 4107–4110.
[68] Y. Tao, Y. Lin, J. Ren, X. Qu, A dual fluorometric and colorimetric sensor for dopamine based on BSA-stabilized Aunanoclusters, Biosens. Bioelectron. 42 (2013) 41–46.
[69] T. Liu, L. Zhang, H. Song, Z. Wang, Y. Lv, Sonochemical synthesis of Ag nanoclusters: electrogenerated chemiluminescence determination of dopamine, Luminscence 28 (2013) 530–535.
[70] L. Li, H. Liu, Y. Shen, J. Zhang, J.J. Zhu, Electrogenerated chemiluminescence of Au nanoclusters for the detection of dopamine, Anal. Chem. 83 (2011) 661–665.
[71] Z. Gao, A. Agarwal, A.D. Trigg, N. Singh, C. Fang, C.H. Tung, et al., Silicon nanowire arrays for label-free detection of DNA, Anal. Chem. 79 (2007) 3291–3297.
[72] Z. Li, Y. Chen, X. Li, T. Kamins, K. Nauka, R.S. Williams, Sequence-specific label-free DNA sensors based on silicon nanowires, Nano Lett. 4 (2004) 245–247.
[73] F. Patolsky, G. Zheng, C.M. Lieber, Nanowire-based biosensors, Anal. Chem. 78 (2006) 4260–4269.
[74] S. Aravamudhan, N.S. Ramgir, S. Bhansali, Electrochemical biosensor for targeted detection in blood using aligned Au nanowires, Sens. Actuators B Chem. 127 (2007) 29–35.
[75] D.T. McQuade, A.H. Hegedus, T.M. Swager, Signal amplification of a "turn-on" sensor: harvesting the light captured by a conjugated polymer, J. Am. Chem. Soc. 122 (2000) 12389–12390.
[76] Y. Chen, J. Yang, X. Ou, X. Zhang, An organic nanowire–metal nanoparticle hybrid for the highly enhanced fluorescence detection of dopamine, Chem. Commun. 48 (2012) 5883–5885.
[77] N.L. Rosi, C.A. Mirkin, Nanostructures in biodiagnostics, Chem. Rev. 105 (2005) 1547–1562.
[78] H. Su, B. Sun, L. Chen, Z. Xu, S. Ai, Colorimetric sensing of dopamine based on the aggregation of gold nanoparticles induced by copper ions, Anal. Methods 4 (2012) 3981–3986.
[79] Y. Zhang, B. Li, X. Chen, Simple and sensitive detection of dopamine in the presence of high concentration of ascorbic acid using gold nanoparticles as colorimetric probes, Microchim. Acta 168 (2010) 107–113.
[80] J.J. Feng, H. Guo, Y.F. Li, Y.H. Wang, W.Y. Chen, A.J. Wang, Single molecular functionalized gold nanoparticles for hydrogen-bonding recognition and colorimetric detection of dopamine with high sensitivity and selectivity, ACS Appl. Mater. Interfaces 5 (2013) 1226–1231.
[81] Y. Zheng, Y. Wang, X. Yang, Aptamer-based colorimetric biosensing of dopamine using unmodified gold nanoparticles, Sens. Actuators B Chem. 156 (2011) 95–99.
[82] Z. Wang, Y. Bai, W. Wei, N. Xia, Y. Du, Magnetic Fe_3O_4-based sandwich-type biosensor using modified gold nanoparticles as colorimetric probes for the detection of dopamine, Materials 6 (2013) 5690–5699.
[83] B. Kong, A. Zhu, Y. Luo, Y. Tian, Y. Yu, G. Shi, Sensitive and selective colorimetric visualization of cerebral dopamine based on double molecular recognition, Angew. Chem. Int. Ed. Engl. 123 (2011) 1877–1880.
[84] H.C. Lee, T.H. Chen, W.L. Tseng, C.H. Lin, Novel core etching technique of gold nanoparticles for colorimetric dopamine detection, Analyst 137 (2012) 5352–5357.
[85] J.M. Liu, X.X. Wang, M.L. Cui, L.P. Lin, S.L. Jiang, L. Jiao, et al., A promising non-aggregation colorimetric sensor of AuNRs–Ag^+ for determination of dopamine, Sens. Actuators B Chem. 176 (2013) 97–102.
[86] W. Smith, C. Rodger, in: J.M. Chalmers, P.R. Griffiths (Editors), Handbook of Vibrational Spectroscopy, Wiley, West Sussex, 2002.
[87] B. Sharma, R.R. Frontiera, A.I. Henry, E. Ringe, R.P. Van Duyne, SERS: materials, applications, and the future, Mater. Today 15 (2012) 16–25.
[88] J.W. Lim, I.J. Kang, Fabrication of chitosan-gold nanocomposites combined with optical fiber as SERS substrates to detect dopamine molecules, Bull. Korean Chem. Soc. 35 (2014) 25–29.
[89] J.W. Lim, I.J. Kang, Chitosan-gold nano composite for dopamine analysis using Raman scattering, Bull. Korean Chem. Soc. 34 (2013) 237–242.

[90] Y. Choi, J.H. Choi, L. Liu, B.K. Oh, S. Park, Optical sensitivity comparison of multiblock gold–silver nanorods toward biomolecule detection: quadrupole surface plasmonic detection of dopamine, Chem. Mater. 25 (2013) 919–926.
[91] P. Dutta, R.B. Pernites, C. Danda, R.C. Advincula, SPR detection of dopamine using cathodically electropolymerized, molecularly imprinted poly-p-aminostyrene thin films, Macromol. Chem. Phys. 212 (2011) 2439–2451.
[92] A. Vaish, W.S. Liao, M.J. Shuster, J.M. Hinds, P.S. Weiss, A.M. Andrews, Thin gold film-assisted fluorescence spectroscopy for biomolecule sensing, Anal. Chem. 83 (2011) 7451–7456.
[93] C.I. Wang, W.T. Chen, H.T. Chang, Enzyme mimics of Au/Ag nanoparticles for fluorescent detection of acetylcholine, Anal. Chem. 84 (2012) 9706–9712.
[94] Y. Lin, C. Chen, C. Wang, F. Pu, J. Ren, X. Qu, Silver nanoprobe for sensitive and selective colorimetric detection of dopamine via robust Ag–catechol interaction, Chem. Commun. 47 (2011) 1181–1183.
[95] J. Biswal, N. Misra, L.C. Borde, S. Sabharwal, Synthesis of silver nanoparticles in methacrylic acid solution by gamma radiolysis and their application for estimation of dopamine at low concentrations, Radiat. Phys. Chem. 83 (2013) 67–73.
[96] M.H. Nezhad, J. Tashkhourian, J. Khodaveisi, Sensitive spectrophotometric detection of dopamine, levodopa and adrenaline using surface plasmon resonance band of silver nanoparticles, J. Iran. Chem. Soc. 7 (2010) 83–91.
[97] M.R.H. Nezhad, J. Tashkhourian, J. Khodaveisi, M.R. Khoshi, Simultaneous colorimetric determination of dopamine and ascorbic acid based on the surface plasmon resonance band of colloidal silver nanoparticles using artificial neural networks, Anal. Methods 2 (2010) 1263–1269.
[98] M. Kaya, M.R. Volkan, New approach for the surface enhanced resonance Raman scattering (SERRS) detection of dopamine at picomolar (pM) levels in the presence of ascorbic acid, Anal. Chem. 84 (2012) 7729–7735.
[99] Y. Lin, M. Yin, F. Pu, J. Ren, X. Qu, DNA-templated silver nanoparticles as a platform for highly sensitive and selective fluorescence turn-on detection of dopamine, Small 7 (2011) 1557–1561.
[100] J.L. Manzoori, M. Amjadi, J. Soleymani, E. Tamizi, A. Rezamand, A. Jouyban, Determination of deferiprone in urine and serum using a terbium-sensitized luminescence method, Luminescence 27 (2012) 268–273.
[101] J.L. Manzoori, A. Jouyban, M. Amjadi, J. Soleymani, Spectrofluorimetric determination of folic acid in tablets and urine samples using 1, 10-phenanthroline-terbium probe, Luminescence 26 (2011) 106–111.
[102] A.M. Alam, M. Kamruzzaman, S.H. Lee, Y.H. Kim, S.Y. Kim, G.M. Kim, et al., Determination of catecholamines based on the measurement of the metal nanoparticle-enhanced fluorescence of their terbium complexes, Microchim. Acta 176 (2012) 153–161.
[103] M. Ahamed, M.S. AlSalhi, M. Siddiqui, Silver nanoparticle applications and human health, Clin. Chim. Acta 411 (2010) 1841–1848.
[104] C. Beer, R. Foldbjerg, Y. Hayashi, D.S. Sutherland, H. Autrup, Toxicity of silver nanoparticles-Nanoparticle or silver ion?, Toxicol. Lett. 208 (2012) 286–292.
[105] J. Gao, M.S. Sepúlveda, C. Klinkhamer, A. Wei, Y. Gao, C.T. Mahapatra, Nanosilver-coated socks and their toxicity to zebrafish (Daniorerio) embryos, Chemosphere 119 (2015) 948–952.
[106] L. Šiller, M.L. Lemloh, S. Piticharoenphun, B.G. Mendis, B.R. Horrocks, F. Brümmer, et al., Silver nanoparticles toxicity in sea urchin Paracentrotus lividus, Environ. Pollut. 178 (2013) 498–502.
[107] O. Bondarenko, K. Juganson, A. Ivask, K. Kasemets, M. Mortimer, A. Kahru, Toxicity of Ag, CuO and ZnO nanoparticles to selected environmentally relevant test organisms and mammalian cells invitro, Arch. Toxicol. 87 (2013) 1181–1200.
[108] E.J. Park, J. Yi, Y. Kim, K. Choi, K. Park, Silver nanoparticles induce cytotoxicity by a Trojan-horse type mechanism, Toxicol. In Vitro 24 (2010) 872–878.
[109] S.B. Nimse, T. Kim, Biological applications of functionalized calixarenes, Chem. Soc. Rev. 42 (2013) 366–386.
[110] N. Korbakov, P. Timmerman, N. Lidich, B. Urbach, A. Sa'ar, S. Yitzchaik, Acetylcholine detection at micromolar concentrations with the use of an artificial receptor-based fluorescence switch, Langmuir 24 (2008) 2580–2587.
[111] D.S. Guo, V.D. Uzunova, X. Su, Y. Liu, W.M. Nau, Operational calixarene-based fluorescent sensing systems for choline and acetylcholine and their application to enzymatic reactions, Chem. Sci. 2 (2011) 1722–1734.
[112] T. Jin, Near-infrared fluorescence detection of acetylcholine in aqueous solution using a complex of rhodamine 800 and p-sulfonato-calix [8] arene, Sensors 10 (2010) 2438–2449.
[113] H. Huang, Y. Gao, F. Shi, G. Wang, S.M. Shah, X. Su, Determination of catecholamine in human serum by a fluorescent quenching method based on a water-soluble fluorescent conjugated polymer–enzyme hybrid system, Analyst 137 (2012) 1481–1486.
[114] S. Kim, T. Sakano, A. Tanaka, T. Nagamura, Sensitive, selective and simple serotonin detection method by CT complex formation between hyperbranched viologen polymer and serotonin, Mol. Cryst. Liquid Cryst. 538 (2011) 304–309.
[115] G. Ozturk, S. Alp, S. Timur, Photophysical characterization of fluorescent oxazol-5-one derivatives in PVC and their application as biosensors in the detection of ACh and AChE inhibitor: donepezil, Dyes Pigm. 76 (2008) 792–798.
[116] M.A. Brun, K.T. Tan, R. Griss, A. Kielkowska, L. Reymond, K. Johnsson, A semisynthetic fluorescent sensor protein for glutamate, J. Am. Chem. Soc. 134 (2012) 7676–7678.
[117] A. Masharina, L. Reymond, D. Maurel, K. Umezawa, K. Johnsson, A fluorescent sensor for GABA and synthetic GABAB receptor ligands, J. Am. Chem. Soc. 134 (2012) 19026–19034.
[118] A.E. Poliakov, A.V. Dumshakova, S.V. Muginova, T.N. Shekhovtsova, A peroxidase-based method for the determination of dopamine, adrenaline, and α-methyldopa in the presence of thyroid hormones in pharmaceutical forms, Talanta 84 (2011) 710–716.
[119] B.J. Melde, B.J. Johnson, P.T. Charles, Mesoporous silicate materials in sensing, Sensors 8 (2008) 5202–5228.
[120] M. Hasanzadeh, N. Shadjou, M. de la Guardia, M. Eskandani, P. Sheikhzadeh, Mesoporous silica-based materials for use in biosensors, Trends Analyt. Chem. 33 (2012) 117–129.
[121] M. Hasanzadeh, N. Shadjou, E. Omidinia, M. Eskandani, M. de la Guardia, Mesoporous silica materials for use in electrochemical immunosensing, Trends Analyt. Chem. 45 (2013) 93–106.
[122] I.I. Slowing, B.G. Trewyn, S. Giri, V.Y. Lin, Mesoporous silica nanoparticles for drug delivery and biosensing applications, Adv. Funct. Mater. 17 (2007) 1225–1236.
[123] C. Yu, M. Luo, F. Zeng, F. Zheng, S. Wu, Mesoporous silica particles for selective detection of dopamine with β-cyclodextrin as the selective barricade, Chem. Commun. 47 (2011) 9086–9088.
[124] Z. Jiang, Y. Fan, M. Chen, A. Liang, X. Liao, G. Wen, et al., Resonance scattering spectral detection of trace Hg^{2+} using aptamer-modified nanogold as probe and nanocatalyst, Anal. Chem. 81 (2009) 5439–5445.
[125] Z. Jiang, X. Liao, A. Deng, A. Liang, J. Li, H. Pan, et al., Catalytic effect of nanogold on Cu (II)–N_2H_4 reaction and its application to resonance scattering immunoassay, Anal. Chem. 80 (2008) 8681–8687.
[126] L. Kong, Z. Liu, X. Hu, S. Liu, Interaction of polymyxin B with ds-DNA, and determination of DNA or polymyxin B via resonance Rayleigh scattering and resonance non-linear scattering spectra, Microchim. Acta 173 (2011) 207–213.
[127] J.X. Dong, N.B. Li, H.Q. Luo, The formation of zirconium hexacyanoferrate (II) nanoparticles and their application in the highly sensitive determination of dopamine based on enhanced resonance Rayleigh scattering, Anal. Methods 5 (2013) 5541–5548.
[128] L. Guo, Y. Zhang, Q. Li, Spectrophotometric determination of dopamine hydrochloride in pharmaceutical, banana, urine and serum samples by potassium ferricyanide-Fe (III), Anal. Sci. 25 (2009) 1451–1455.
[129] J.X. Dong, W. Wen, N.B. Li, H.Q. Luo, Determination of dopamine at the nanogram level based on the formation of Prussian blue nanoparticles by resonance Rayleigh scattering technique, Spectrochim. Acta [A.] 86 (2012) 527–532.
[130] S. Das, S. Guha, A. Banerjee, S. Lohar, A. Sahana, D. Das, 2-(2-Pyridyl) benzimidazole based Co (ii) complex as an efficient fluorescent probe for trace level determination of aspartic and glutamic acid in aqueous solution: a displacement approach, Org. Biomol. Chem. 9 (2011) 7097–7104.